Fuel Processing Technology

Effect of CO2 on HCl removal from syngas using normal and modified Ca-based hydrotalcites: a comparative study

--Manuscript Draft--

Manuscript Number:	FUPROC-D-23-01543R1
Article Type:	Research Paper
Keywords:	Ca-Mg-Al-CO3; CO2; HCl removal; TGA; Adsorption kinetics
Corresponding Author:	Baosheng Jin Southeast University Nanjing, Jiangsu Province China
First Author:	Songshan Cao
Order of Authors:	Songshan Cao
	Jun Cao
	Hualun Zhu
	Yaji Huang
	Baosheng Jin
	Massimiliano Materazzi
Abstract:	MSW pyrolysis and gasification technologies have been recognized as effective means to enhance the resource utilization of MSW and promote a circular economy. However, the presence of HCl gas can significantly impact the quality and application of syngas. To maximize syngas resource utilization, develop highly efficient HCl adsorbent, this study investigates the performance and mechanism of HCl removal from syngas using a conventional hydrotalcite (Mg-Al-CO3) and modified Ca-based hydrotalcite (Ca-Mg-Al-CO3). The impact of CO2, a component naturally presents in syngas, on the performance of both materials, were also investigated. Characterization techniques, including XRD, TGA, SEM, and analysis of pore properties and specific surface area, were employed to understand the underlying reaction mechanism. The results demonstrated that the performance of Ca-Mg-Al-CO3 was significantly superior to that of conventional Mg-Al-CO3 sorbents, particularly in the presence of CO2 However, the presence of CO2 had a detrimental impact on the performance of Ca-Mg-Al-CO3 in HCl removal, and this effect became increasingly pronounced with higher concentrations of CO2. TGA results revealed a competitive relationship between HCl and CO2 during the adsorption process. Additionally, the fitting results of adsorption kinetics suggested that the adsorption reaction of HCl and CO2 by Ca-Mg-Al-CO3 followed multiple rate-controlling mechanisms.
Suggested Reviewers:	Denian Li, Doctor Professor, Guangzhou Institute of Energy Conversion lidn@ms.giec.ac.cn
	Hong Yao, Doctor Professor, Huazhong University of Science and Technology hyao@hust.edu.cn
	Hao Liu, Doctor Professor, University of Nottingham liu.hao@nottingham.ac.uk
	Wen Yang, Doctor Professor, Guilin University of Technology yangwen167@163.com
	Shengping Wang, Doctor Professor, Tianjin University spwang@tju.edu.cn
Response to Reviewers:	

Dear Editor:

I am pleased to submit an original research manuscript entitled 'Effect of CO_2 on HCl removal from syngas using normal and modified Ca-based hydrotalcites: a comparative study' on behalf of all authors. We are submitting it for consideration as a research article in *FUEL PROCESSING TECHNOLOGY*.

This study investigates the performance and mechanism of HCl removal from waste derived syngas using a conventional hydrotalcite (Mg-Al-CO_3) and modified Ca-based hydrotalcite (Ca-Mg-Al-CO_3), analyzing the impact of CO_2, naturally present in syngas, on both materials. The results demonstrated that the performance of Ca-Mg-Al-CO_3 was significantly superior to that of conventional Mg-Al-CO_3 sorbents when CO_2 is present. According to the in-situ TGA results, a competitive relationship between HCl and CO_2 was observed during the adsorption process. Initially, the adsorption rate of HCl surpassed that of CO_2, but the adsorption capacity of CO_2 is significantly higher, likely due to its significantly higher concentration, which was hundreds of times greater than that of HCl. This concentration disparity serves as an additional factor contributing to the observed decline in the performance of HCl removal. Additionally, the fitting results of adsorption kinetics revealed that the adsorption reaction of HCl and CO_2 by Ca-Mg-Al-CO_3 followed multiple rate-controlling mechanisms.

We believe that this work will increase the understanding of HCl removal and therefore prompt researchers to test their catalysts under more realistic conditions. We believe this is a good match with the *FUEL PROCESSING TECHNOLOGY*, where the most relevant literature on this topic is published.

The authors guarantee that none of the content in the paper has been published or is under consideration for publication elsewhere. All authors have approved the manuscript and have agreed to this submission. This paper is the original work of the all authors.

Thank you very much for your consideration.

Yours faithfully,

Songshan Cao

Corresponding author:
1. Baosheng Jin
Corresponding address and other information is as follows：
Address:
Key Laboratory of Energy Thermal Conversion and Control of Ministry of Education, School of Energy and Environment, Southeast University, Nanjing, 210096, Jiangsu province China.
E-mail: bsjin@seu.edu.cn
Tel.: +86 18761892386

2. Massimiliano Materazzi

Corresponding address and other information is as follows：

Address:

Department of Chemical Engineering, University College London, London WC1E 7JE, United Kingdom.

E-mail: massimiliano.materazzi.09@ucl.ac.uk

Tel.: +44 7837626421

The references of potential reviewers:

[1] **D. Li,** J. Yang, Y. Zhao, H. Yuan, Y. Chen, Ultra-highly porous carbon from Wasted soybean residue with tailored porosity and doped structure as renewable multi-purpose absorbent for efficient CO_2, toluene and water vapor capture, Journal of Cleaner Production, 337 (2022) 130283.

[2] E. Garcia, I.F. Ejim, **H. Liu,** Thermogravimetric analysis of co-combustion of a bituminous coal and coffee industry by-products, Thermochimica acta, 715 (2022) 179296.

[3] Y. Ren, C. Cao, H. Hu, S. Lei, X. Yuan, X. Li, **H. Yao,** Transformation behavior and fate of chlorine in polychloroprene (PCP) during its pyrolysis, Fuel, 317 (2022) 123573.

[4] Y. Feng, B. Xiao, K. Bo, H. Chen, **W. Yang,** Controllable preparation of porous Ca-Mg-Al hydroxides based adsorbents and their CO_2 adsorption performances, Ferroelectrics, 594 (2022) 44-56.

[5] T. Jiang, F. Xiao, Y. Zhao, **S. Wang**, X. Ma, High-temperature CO_2 sorbents with citrate and stearate intercalated CaAl hydrotalcite-like as precursor, Chinese Journal of Chemical Engineering, 50 (2022) 177-184.

Dear editor and reviewers,

The authors gratefully acknowledge the valuable comments made by the reviewers. We have studied their comments carefully and have made corrections, which we hope meet with their approval.

Editor and Reviewer comments:

Editor:

The manuscript needs to be re-written and re-reviewed.

We appreciate your feedback on our manuscript. We take your comments seriously and are committed to improving the quality of our work. We understand the importance of delivering a well-written and well-structured manuscript.

We thank you for your guidance and look forward to the opportunity to provide a significantly improved manuscript for your consideration.

Reviewer #1:

We sincerely appreciate your time and efforts in reviewing our manuscript titled "*Effect of CO_2 on HCl removal from syngas using normal and modified Ca-based hydrotalcites: a comparative Study*". We sincerely appreciate your provision for allowing us to undertake some necessary revision of the manuscript. Your insightful suggestions have not only been fully considered but have been the catalyst for a sweeping and

transformative overhaul of the manuscript.

We have carefully crafted detailed responses to each of your insightful suggestions and comments, showcasing the depth and breadth of the revisions undertaken. We look forward to presenting you with a significantly enhanced version of our manuscript, refined to embody a higher standard of scholarly work. We greatly appreciate your feedback, and we would like to address your comments in a comprehensive, point-by-point manner as follows:

Issue 1:

As shown in the schematic diagram of the setup, there is a condenser before the HCl analyzer. There is a concern that part of HCl will condense in this step can cause the deviation of the measurement of the analyzer.

Response 1:

Thank you for your careful comments. Due to the operating condition limitations of the HCl analyzer from Signal Group Ltd., UK, in order for the HCl analyzer to operate normally and ensure measurement accuracy, the temperature of the introduced HCl gas must be maintained below 50°C. Therefore, we discussed this issue with engineers from Signal Group Ltd., and as shown in Figure 3A, a condenser has been added. This condenser is used to process gaseous HCl, preventing it from condensing when it enters the analyzer. The purpose of this condenser is to cool and convert HCl gas back into a gaseous state, ensuring accurate measurements. While some condensation of HCl may occur, the design and operation of the condenser aim to minimize this phenomenon and

maintain measurement accuracy. Furthermore, we will conduct regular inspections and maintenance on the condenser to ensure its proper functioning and to avoid significant deviations in measurement results.

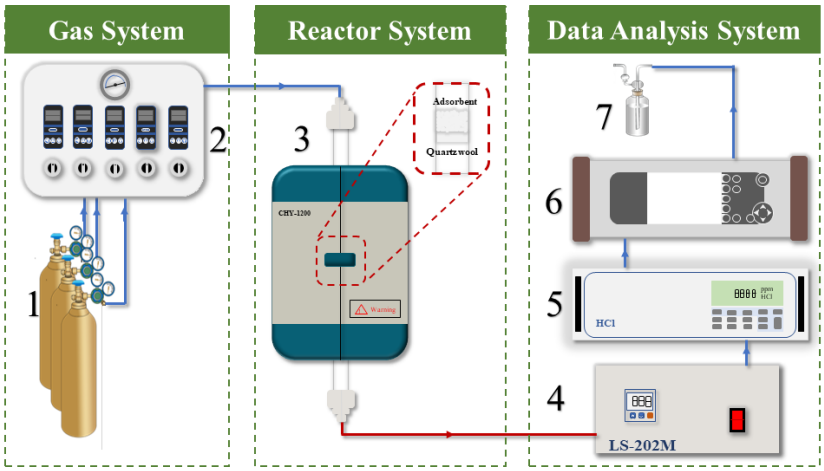

1. Gas cylinder; 2. Mass flowmeter; 3. Reactor; 4. LJ-202M condenser; 5. HCl analyzer; 6. Flue gas analyzer; 7. Gas-washing bottle

Figure3A. The schematic diagram of experiments

Issue 2:

The presence of CO_2 could possibly affect the accurate measurement of HCl (cross interface between CO_2 and HCl). Blank tests should be conducted without the adsorbents to check the stability of the HCl measurement under different CO_2 concentrations.

Response 2:

Thank you for your comment. Regarding the HCl analyzer, we communicated our requirements to the engineer during the equipment procurement process, emphasizing that HCl should not be affected by other gases such as CO_2, CO, O_2, and H_2 during

testing. To address this, the manufacturer added an internal data processing module to the device. Before conducting our experiments, we also performed a blank test involving both CO_2 and HCl to ensure that there was no mutual interference. The relevant test data are as follows: Initially, we measured HCl using the HCl analyzer. Once the HCl gas had stabilized, we introduced CO_2 gas, gradually increasing the concentration from 0% to 25%. The experimental results confirmed that different concentrations of CO_2 had no impact on the HCl analyzer.

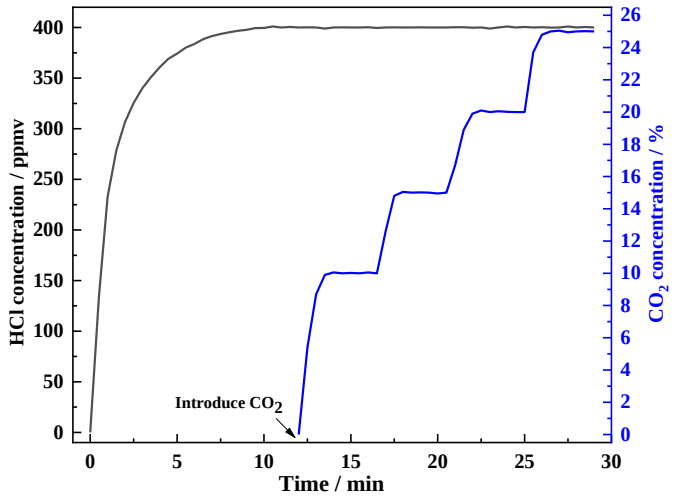

The blank test of the impact of CO_2 concentration on HCl concentration

Issue 3:

In Figure 7D, the HCl capacity was 217.9 for Ca-Mg-Al-CO3 at 300C and 20% CO2. Yet in Figure 8D under the same operation condition, the HCl capacity was 271.9. The repeatability seems questionable. The realizability and repeatability of the data should be double checked for the whole manuscript.

Response 3:

We apologize for this mistake. After a thorough review, we have recalculated the HCl capacity, and it has been confirmed to be 217.9 $mg \cdot g^{-1}$ for Ca-Mg-Al-CO_3 at 300°C and

20% CO_2. The manuscript has been updated with this corrected data."

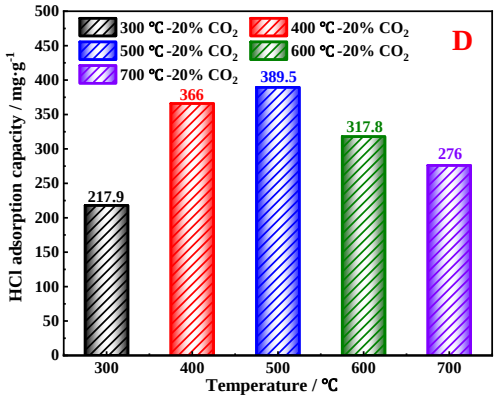

Fig. 8 the maximum breakthrough chlorine capacity

This behavior is further supported by Fig.8 D, which indicates that the maximum breakthrough chlorine capacity of Ca-Mg-Al-CO_3 increased from 217.9 mg/g to 389.5 mg/g as the reaction temperature increased from 300 to 500 ℃, then decreased from 389.5 mg/g to 276 mg/g as the reaction temperature further increased from 500 to 700 ℃

Issue 4:

The authors indicated that the pore structure variation at different temperatures would cause the optimum removal capacity of HCl at 500C. Yet no evidence was provided. The surface area, pore size distribution, and surface morphology at different temperatures should be provided to support their assumptions.

Response 4:

According to the comment of the reviewer, we would like to provide a detailed explanation regarding the adsorption mechanism as follows, and we have added the explanation to the manuscript.

The surface morphology, pore size distribution, and specific surface area of Ca-Mg-Al-CO_3 at different temperatures were shown in Fig.10. As shown in the SEM images of Fig 10 A-E, with increase of temperature, surface morphology of Ca-Mg-Al-CO_3 becomes fluffy, however, there is a sintering phenomenon when the temperature exceeds 500 ℃. In Fig.10 F, the pores of Ca-Mg-Al-CO_3 are mainly mesopores. With the increase of temperature, the number of pores first increases and then decreases, and pores develop towards larger pores, the pore structure is optimal at 500 ^oC. Therefore, as shown in Fig. 10 G, the specific surface area also first increases and then decreases, the specific surface area was larger at 500 ℃, 58.1 m^2/g. The large specific surface area provides more active sites, facilitates the availability of more active sites. Above results further illustrated that why the Ca-Mg-Al-CO_3 exhibits excellent performance in removing HCl at 500 ^oC.

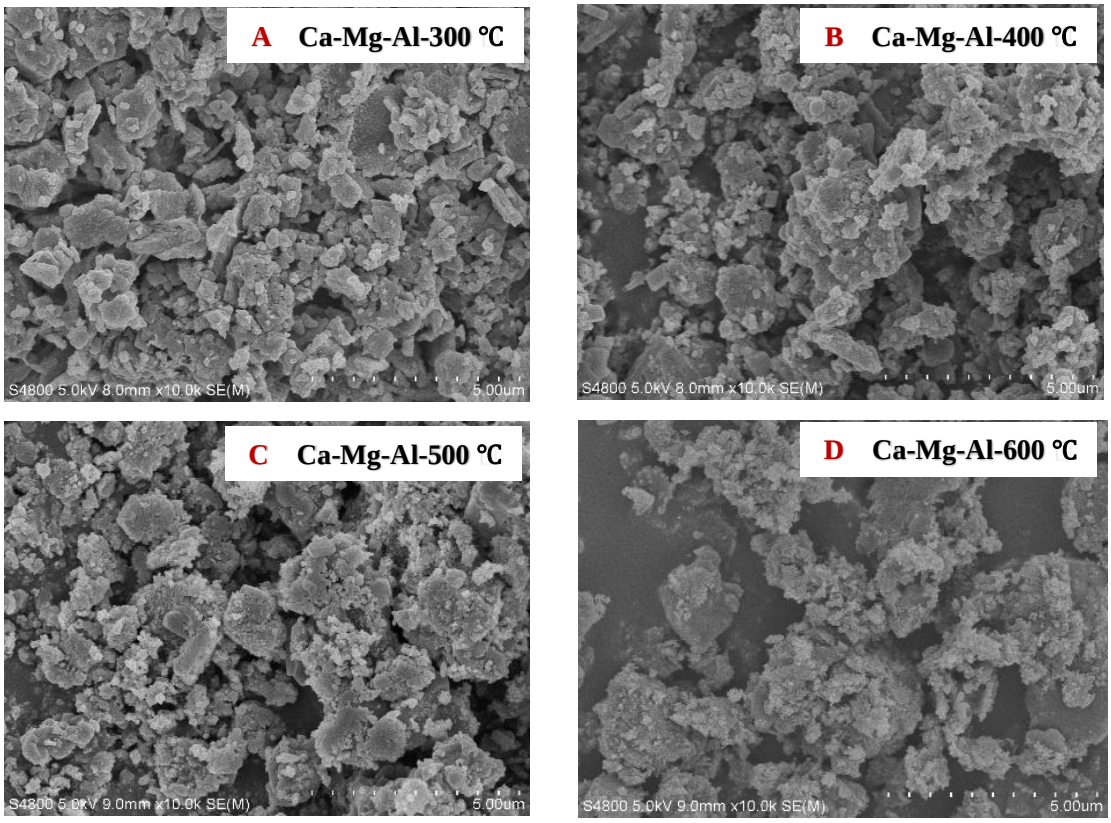

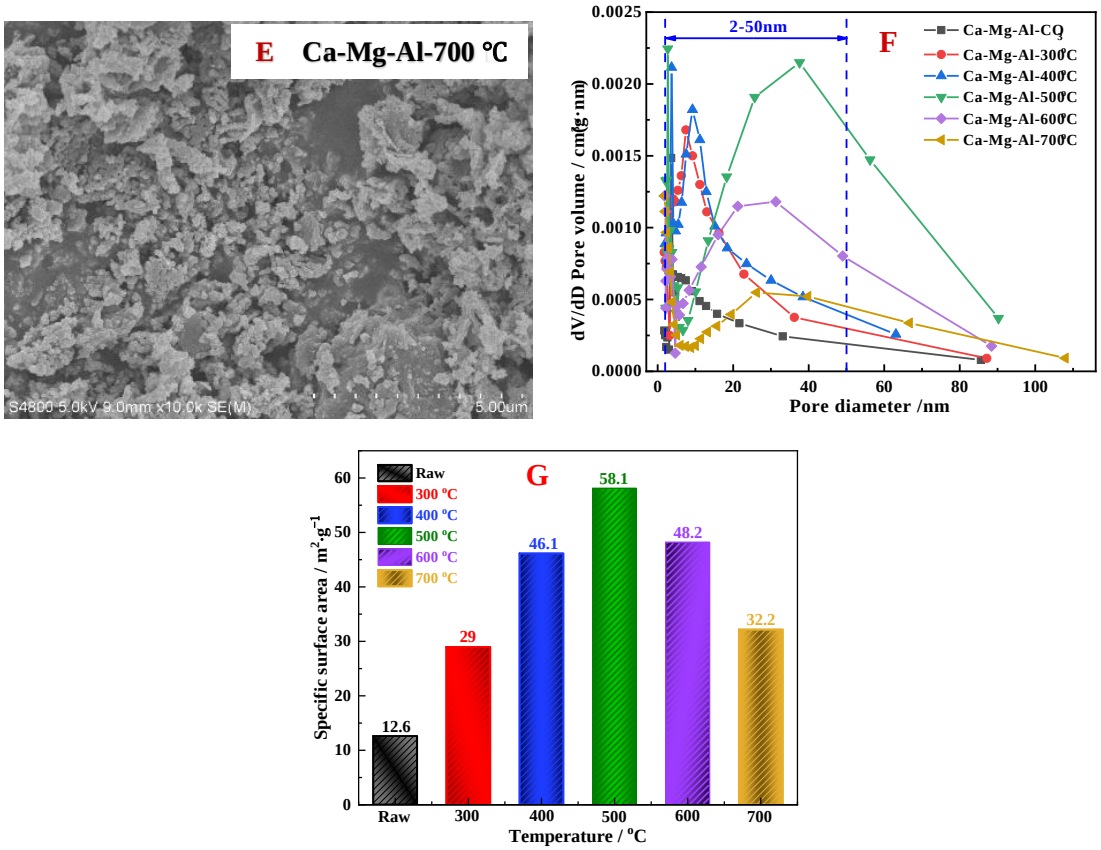

Fig. 10 The surface morphology, pore size distribution, and specific surface area of Ca-Mg-Al-CO_3 at different temperatures (A-E: Surface morphology; F: Pore size distribution; G: Specific surface area)

Issue 5:

Why the intra-particle diffusion model, Elovich model and Bangham model were selected for fitting study? All of them are faired to present the q variation at the later adsorption stage, even though they showed R2 higher than 0.9. The conclusion made based on this kinetic study may not be reasonable.

Response 5:

Thank you for your comment. We reference the literatures and then selected five kinetic fitting models for gas-solid reaction, therefore, we reanalyzed the data and drew new

figures. Based on the results of fitting, the fitting results of the PSO is the best, indicating that the chemical adsorption is main reaction mechanism throughout the entire reaction process, and chemical adsorption involves electron sharing or electron transfer between Ca-Mg-Al-CO_3 and CO_2, HCl. Other fitting results also are good in the early stage of the reaction, showing that the reaction was controlled by multiple rate-controlling mechanisms. The new results are as follows,

3.6 Apparent adsorption kinetic

The apparent adsorption kinetic models mainly include kinetic control type and diffusion control type. The diffusion control type includes Intra-particle diffusion model, which describes gas film or intra-particle diffusion as a rate-controlling step. The commonly used kinetic control models are Pseudo-first-order model (PFO), Pseudo-second-order model (PSO), Elovich model and Bangham model, all of which describe the kinetic adsorption process of surface adsorption or surface chemical reactions as rate-controlling steps. The experimental results of HCl removal by Ca-Mg-Al-CO_3 at different CO_2 concentrations were analyzed using the above models, and the fitting results of adsorption kinetics are presented in Fig. 12.

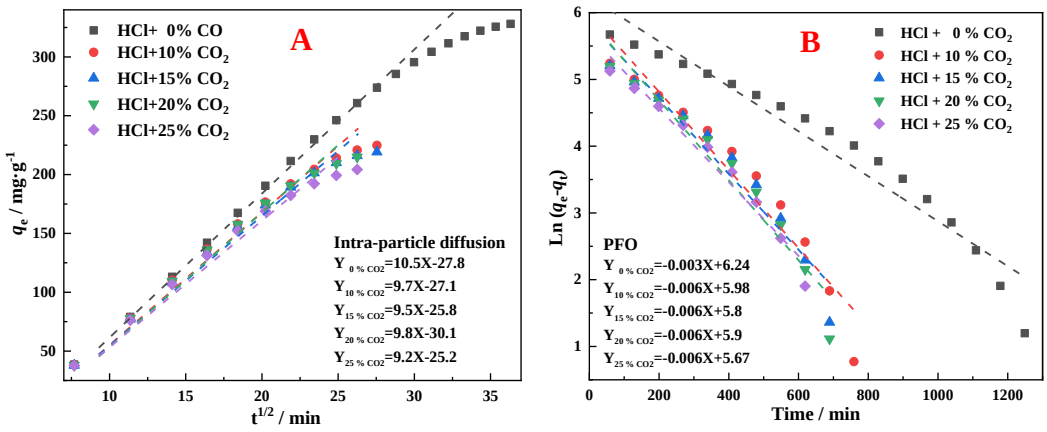

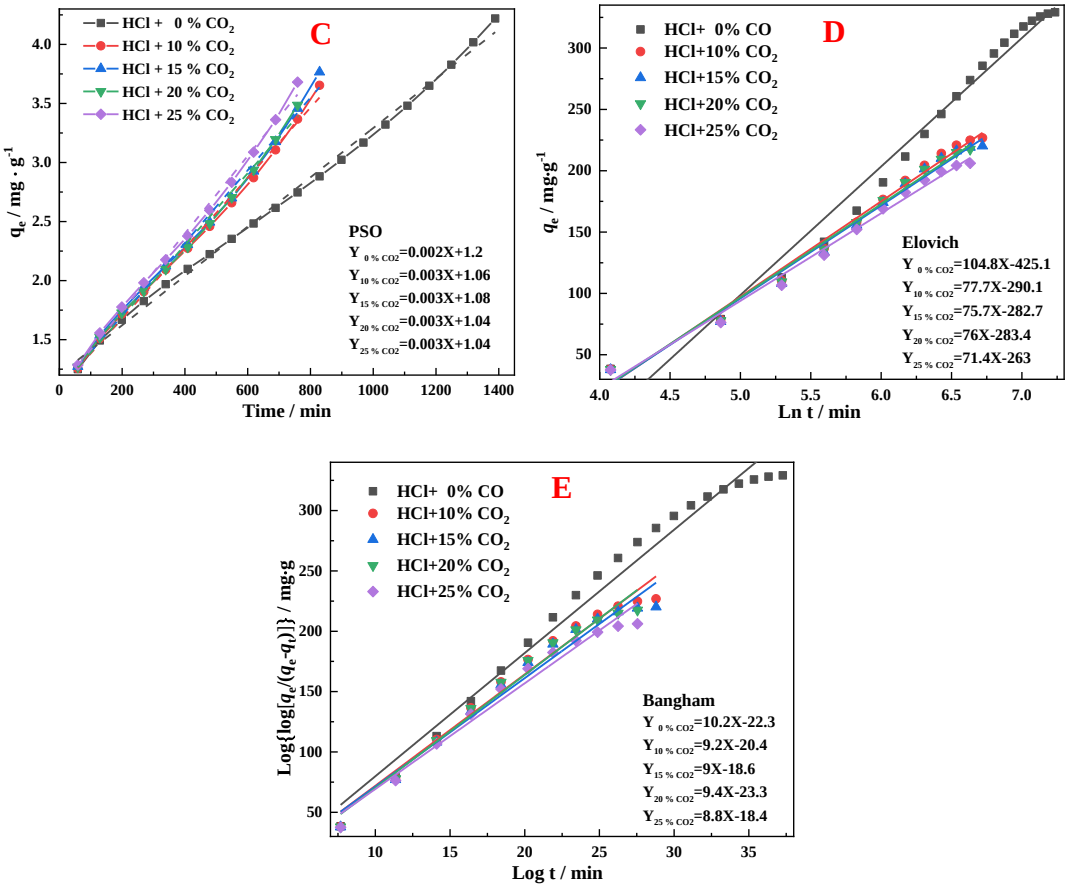

Fig. 12 The fitting results of different adsorption kinetic model (A: Intra-particle diffusion model; B: Pseudo-first-order model (PFO), C: Pseudo-second-order model; D: Elovich model; E: Bangham model)

As depicted in Fig. 12 and the correlation coefficients (R^2) summarized in Table 2, based on the fitting result of the intra-particle diffusion model, the fitted line does not pass through the origin and did not exhibit a linear relationship, the R^2 values are more than 0.98, indicating that diffusion control is not the solely governed by single rate-determining steps. The fitting results of 4 kinetic control types showed a relatively best agreement with the PSO model, the R^2 values exceed 0.99. The result illustrates that the chemical adsorption is main reaction mechanism in whole reaction process, and chemical adsorption involves electron sharing or electron transfer between Ca-Mg-Al-

CO_3 and HCl, CO_2. Compared to PSO model. Although the R^2 values of other 3 adsorption kinetic models were slightly lower than that of the PSO model, all models exhibited correlation coefficients above 0.97, as shown in Fig. 12B, D and E, there a good fitting result in the early stage of the reaction, indicating it is controlled by multiple control steps in the early stage of the reaction.

Table. 2 The correlation coefficients (R^2) of different adsorption kinetic models

Model	0% CO_2 +HCl	10% CO_2 + HCl	15% CO_2 + HCl	20% CO_2 +HCl	25% CO_2 +HCl
Intra-particle diffusion	0.983	0.985	0.983	0.987	0.985
PFO	0.94	0.933	0.946	0.943	0.968
PSO	0.996	0.996	0.994	0.996	0.996
Elovich	0.98	0.988	0.987	0.989	0.99
Bangham	0.977	0.976	0.972	0.978	0.974

Issue 6:

Can the absorbent be regenerated for cyclic utilization?

Response 6:

Thank you for your comment. Regeneration of the absorbent is indeed a critical aspect, and we appreciate your interest in this matter.

According to the properties of hydrotalcite, which include its layered structure, exchangeability of interlayer anions, thermal stability, and memory effect, it is known

that under certain conditions, hydrotalcite can be restored to its original form. However, the effectiveness of the restoration process is dependent on the reaction temperature. If the temperature exceeds a specific threshold, the structure of hydrotalcite may be irreversibly altered, making restoration challenging. Based on our experiments, we have determined that the Mg-Al-CO_3 sample retained a significant portion of its hydrotalcite structure with only minimal decomposition under 400^{o}C. To regenerate the sorbent, an anion exchange process was employed as depicted in *React*. 1 and 2.

$Mg_{3n}Al_nO_{9n/2} + (n/2)CO_3^{2-} + (9n/2)H_2O \rightarrow Mg_{3n}Al_n(OH)_{8n}(CO_3)_{n/2} + OH^-$ *(React.* 1)

$Mg_{3n}Al_n(OH)_2Cl_n + (n/2)CO_3^{2-} + mH_2O \rightarrow Mg_{3n}Al_n(OH)_2(CO_3)_{2n}\bullet mH_2O + nCl^-$ *(React.* 2)

To replenish the missing water and carbonate ions in the product, in the test, the product was immersed in a sodium carbonate solution of a specific concentration. Then the repaired Mg-Al-400 was obtained by calcining the product at 400 ^{o}C. This repaired sorbent was then subjected to breakthrough tests to remove HCl, under the following reaction conditions: an HCl concentration of 400 ppmv, a reaction temperature of 300 ^{o}C, and a gas flow of 500 ml/min. The experimental results indicate that even after cycling the sorbent three times, the adsorption capacity of HCl remained at approximately 50%. However, a subsequent decline in performance was observed. There are two main reasons for the decrease in performance. Firstly, according to *React.* 1 and 2, the restoration of Mg-Al-CO_3 and the subsequent desorption of Cl^- could not reach 100%. Secondly, a portion of the Mg^{2+} may have already reacted with Cl^- to generate $MgCl_2$. Therefore, the recovery is not 100% and the crystallinity is reduced

during the recovery process.

Regarding calcium based modified hydrotalcite, the structure of Ca-Mg-Al-CO_3 is similar to Mg-Al-CO_3, suggesting the potential for regeneration. We apologize for not conducting a detailed study on the regeneration ability of Ca-Mg-Al-CO_3. In our future work, we plan to explore and provide comprehensive insights into the regeneration and recyclability of hydrotalcites for HCl removal. Consequently, we are actively exploring improved methods to enhance the recyclability of the sorbent, aiming to achieve environmental sustainability and cost reduction.

We appreciate your feedback, and we will ensure that the regeneration experiments and their outcomes are included in our future work to provide a comprehensive understanding of the regeneration and cycle usage of hydrotalcites for HCl removal.

Reviewer #2:

We would like to express our sincere gratitude for your time and effort invested in the review of our manuscript titled "*Effect of CO_2 on HCl removal from syngas using normal and modified Ca-based hydrotalcites: a comparative Study*". We are thankful for your consideration in allowing us to make essential revisions to our manuscript. Your valuable suggestions have not only been thoroughly taken into account but have also played a pivotal role in instigating a comprehensive transformation of our paper.

We have diligently prepared detailed responses to each of your insightful recommendations and comments, illustrating the extensive scope of the revisions that have been carried out. We are eagerly looking forward to presenting you with an

upgraded version of our manuscript, refined to meet the highest standards of academic work. Your feedback is highly appreciated, and we are committed to addressing your comments meticulously, item by item, as outlined below:

Issue 1:

I do not like this abstract. It did not tell the reader why you did this work, and which methodology you take to do the research. I mean, this abstract is more like a conclusion, rather than an abstract.

Response 1:

Thank you for your comment, we have modified abstract.

MSW pyrolysis and gasification technologies have been recognized as effective means to enhance the resource utilization of MSW and promote a circular economy. However, the presence of HCl gas can significantly impact the quality and application of syngas. To maximize syngas resource utilization, develop highly efficient HCl adsorbent, this study investigates the performance and mechanism of HCl removal from syngas using a conventional hydrotalcite (Mg-Al-CO_3) and modified Ca-based hydrotalcite (Ca-Mg-Al-CO_3). The impact of CO_2, a component naturally presents in syngas, on the performance of both materials, were also investigated. Characterization techniques, including XRD, TGA, SEM, and analysis of pore properties and specific surface area, were employed to understand the underlying reaction mechanism. The results demonstrated that the performance of Ca-Mg-Al-CO_3 was significantly superior to that of conventional Mg-Al-CO_3 sorbents, particularly in the presence of CO_2 However, the

presence of CO_2 had a detrimental impact on the performance of Ca-Mg-Al-CO_3 in HCl removal, and this effect became increasingly pronounced with higher concentrations of CO_2. TGA results revealed a competitive relationship between HCl and CO_2 during the adsorption process. Additionally, the fitting results of adsorption kinetics suggested that the adsorption reaction of HCl and CO_2 by Ca-Mg-Al-CO_3 followed multiple rate-controlling mechanisms.

Issue 2:

Pages missing.

Response 2:

Thank you for your comment, we have added page numbers and verified the manuscript to ensure that the page numbers are accurate.

Issue 3:

"According to the in-situ TGA results,.." But TGA are always in-situ, right?

Response 3:

Thank you for your comment, we have changed in-situ TGA to TGA, and deleted ‘in-situ’.

Issue 4:

Please reorganize the introduction to highlight the novelty and contribution of this work.

(1) Please consider the significance of studying the CO2 concentration on the removal of HCl. Can you control the CO2 concentration in the pyrolysis gas??

Response 4:

Thank you for your comment, based on your suggestion, we have reorganized the introduction to highlight the novelty and contribution. The modification content is as follows,

It is important to note that CO_2, a non-combustible gas, is present in syngas at significantly higher concentrations than HCl. CO_2 is a key component in various processes, including the water-gas shift reaction, producing CO and so on , It has been established that hydrotalcite can adsorb CO_2 effectively.[42, 43] CO_2 is also confirmed to be adsorbed by hydrotalcite [44, 45]. Therefore, both HCl and CO_2 can be adsorbed by hydrotalcite. Especially in the case of Ca-Mg-Al-CO_3, it exhibits remarkable capabilities in adsorbing CO_2 due to the generation of calcium-containing oxide at mid-high temperatures[46, 47]. Consequently, the presence of CO_2 may influence the performance of HCl removal using hydrotalcite and Ca-Mg-Al-CO_3, although the specific effect tendency is not yet well understood. Although some studies have reported on the effect of CO_2 on HCl removal using other calcium-based compounds such as CaO, $Ca(OH)_2$ and $CaCO_3$[48, 49], it should be noted that the research objectives and operating conditions varied, resulting in inconsistent results. Therefore, when studying the performance of HCl removal in syngas, the effect of CO_2 on HCl removal using hydrotalcite and hydrotalcite-like compounds should not be overlooked. Surprisingly, there is a lack of research focusing on the characteristics of HCl removal using hydrotalcite and hydrotalcite-like compound in the presence of CO_2. Therefore, it is necessary to analyze the effect and mechanism of CO_2 on HCl removal by adsorbent.

Obtaining the impact tendency of CO_2 on HCl removal by hydrotalcite is crucial for ensuring the production of high-quality syngas and expanding the applications of syngas in various fields.

Issue 5:

Line 49. as small footprint and higher energy efficiencies, . but footprint of whom?? CO2 footprint???> If it weren't for the pressure of carbon footprint, these solid wastes could all be landfilled and composted, so there's no need for such a complex disposal process. You can start by rewriting the introduction from the perspective of energy consumption and CO2 emission reduction. At present, the background and significance of this MS version is not enough persuasive. In addition, here the CO2 footprint should cite some related references such as "[1] Integrated CO2 capture and utilization with CaO-alone for high purity syngas production. Carbon Capture Science & Technology 1 (2021) 100001 [2]Use of copper carbonate as corrosion inhibitor for carbon steel in post combustion carbon capture. Carbon Capture Science & Technology.6(2023) 100095"

Response 5:

Thank you for your comment, based on your suggestion, we have made modifications to introduction and added relevant references, including those recommended by you.

The disposal of municipal solid waste (MSW) has become a pressing issue due to rapid growth of human population and associated industrial activities[1]. The proper utilization of MSW can significantly contribute to the goal of carbon emission reduction[2]. The modern waste management strategies prioritize waste minimization,

recycling, and reuse, with landfill disposal considered as the least desirable option to prevent pollution of surface water, groundwater, soil and air, as well as to reduce GHG emissions from the landfill sites. In the background of global carbon neutrality，finding rational ways to utilize MSW is of paramount importance for reducing energy waste and carbon dioxide emissions [3, 4].

…

These technologies not only enable waste disposal while reducing emissions of gaseous pollutants such as NOx and SOx, but also exhibit characteristics such as a small footprint and higher energy efficiencies[8]. Especially in the context of achieving carbon neutrality, the use of pyrolysis and gasification technology for waste processing becomes particularly vital in reducing the pressure of carbon emissions[9, 10].

Issue 6:

Line 72. title case of therefore?

Response 6:

We apologize for this mistake. We have changed ‘therefore’ to ‘Therefore’.

Issue 7:

2.1 Synthetic steps,. Here, there are so many paragraphs that are only one sentence.

Response 7:

Thank you for your comment, we have reorganized section 2.1, which is as follows,

In this study, the chemical reagents of Mg $(NO_3)_2 \cdot 6H_2O$, Al $(NO_3)_3 \cdot 9H_2O$, Ca $(NO_3)_2 \cdot 4H_2O$, NaOH and Na_2CO_3 with analytically pure grade were produced from

Sinopharm Chemical Reagent Co., Ltd. The Mg-Al hydrotalcite containing CO_3^{2-} intercalated (Mg-Al-CO_3), and Ca-based modified hydrotalcite-like (Ca-Mg-Al-CO_3) were synthesized using the coprecipitation method for gaseous HCl removal. The synthetic process is shown in Fig. 2 and the synthetic steps are as follows.

Preparation of Mg-Al-CO_3: (1) According to the molar ratio of Mg/Al=3, $[OH^-]=2([Mg^{2+}]+[Al^{3+}])$ and $[CO_3^{2-}]=1/2[Al^{3+}]$, the corresponding chemical reagents were weighed. (2) The nitrates and two bases were dissolved in ultra-pure water at 60 °C, respectively. (3) The two solutions were dropped into a four-port flask at a certain speed using a peristaltic pump at 60 °C. During this process, the pH value was maintained at 11, and the stirring speed was set at 300 r/min. The resulting mixture was continuously stirred for 2 hours at 60 °C. (4) The obtained substance was subjected to crystal growth for 20 hours at 80 °C. (5) The solid part was washed using ultra-pure water until neutral, dried and grounded. The Mg-Al-CO_3 was obtained, and the particles in size range of 40 to 60 mesh were chosen for subsequent experiments.

Preparation of Ca-Mg-Al-CO_3: The Ca-Mg-Al-CO_3 was prepared with a molar ratio of $Ca^{2+}/Mg^{2+}=(Ca+Mg)^{2+}/Al^{3+}=3$, $[OH^-]=2([(Ca+Mg)^{2+}]+[Al^{3+}])$ and $2[CO_3^{2-}]=[Al^{3+}]$. The step (2) to (5) mentioned above were repeated to obtain Ca-Mg-Al-CO_3, and the particle sizes range was the same as that of Mg-Al-CO_3.

Issue 8:

The Figure 3 should better be moved to the SI.

Response 8:

Thank you for your suggestion. Figure 3 illustrates the schematic diagram of both the HCl removal experiment and the TGA experiment. We believe that Figure 3 is

beneficial for readers to have a clearer understanding of the experimental steps and methods, facilitating a better grasp of the author's experimental intentions.

Issue 9:

Figure 4. The scare bar is Unclear.

Response 9:

Thank you for your comment. Based on the reviewer's feedback, we have made the necessary modifications to Figure 4 and replaced the SEM image to ensure that Figure 4 is clear and visually accurate. We appreciate the reviewer's attention to detail and their valuable feedback.

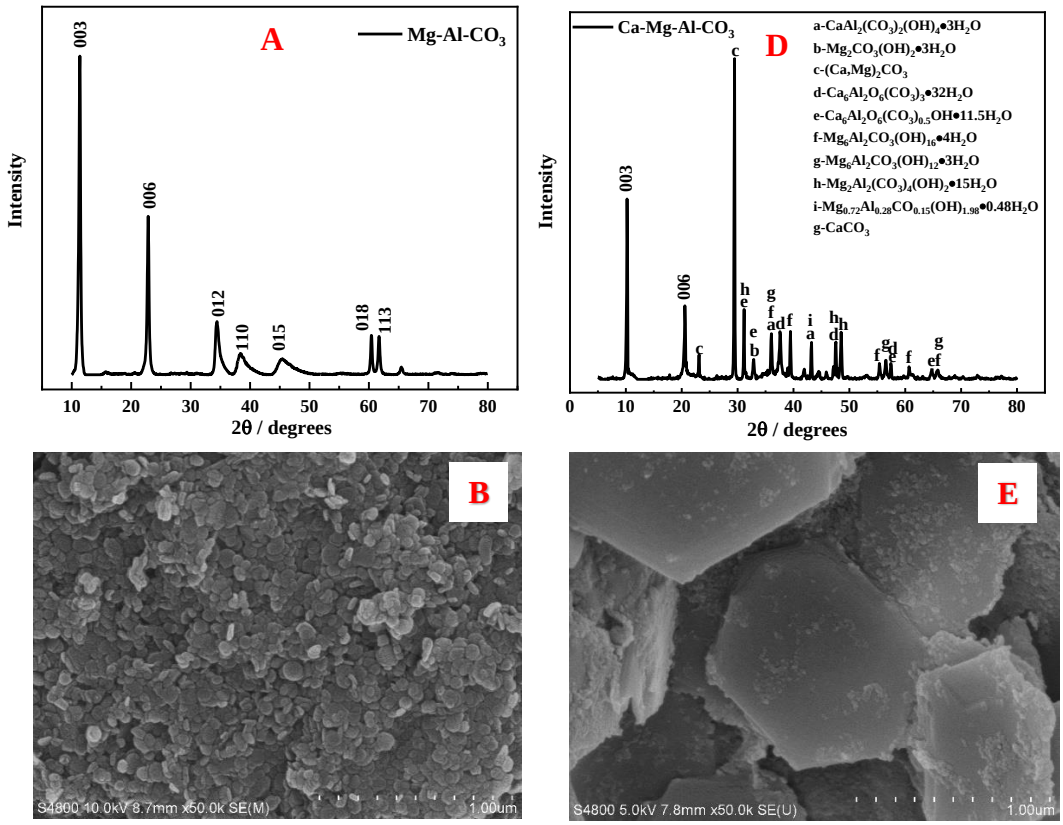

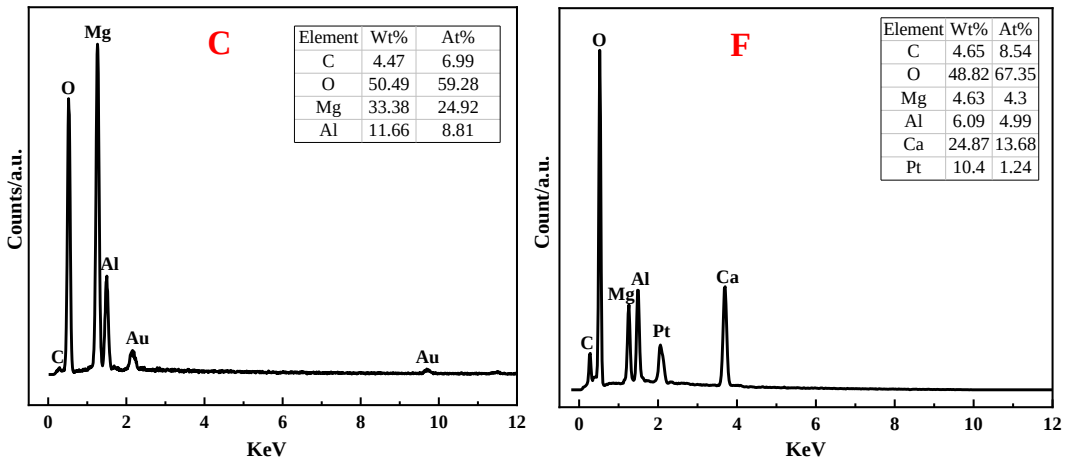

Fig. 4 Characterization of adsorbents (Mg-Al-CO_3: A: XRD pattern, B: SEM image, C: EDS pattern; Ca-Mg-Al-CO_3: D: XRD pattern, E: SEM image, F: EDS pattern)

Issue 10:

The Figures all should better be reorganized. The explanation of the content can be placed below (caption), and it is important to ensure the clarity and aesthetics of the images.

Response 10:

Thank you for your comment. We have addressed your suggestion to enhance the clarity and aesthetics of the figures. Based on the reviewer's feedback, we have made modifications to all figures in the manuscript. An example of the modified figure is shown below (using Fig. 7 as an illustration).

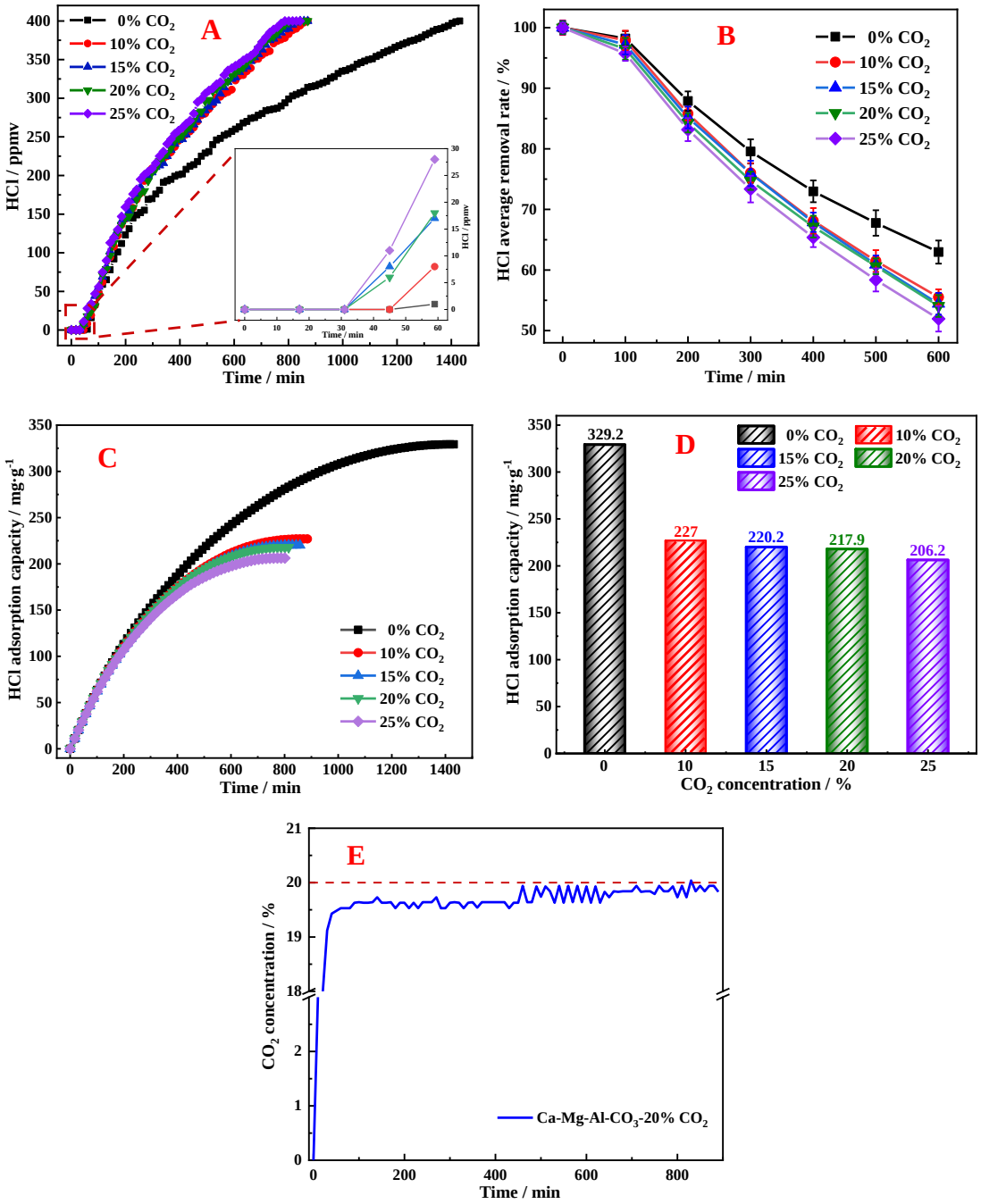

Fig.7 The performance of HCl removal using Ca-Mg-Al-CO_3 under different CO_2 concentrations and the change curve of CO_2 (A: the breakthrough curves; B: the average removal of HCl rate; C: the adsorption chlorine capacity curves; D: the maximum breakthrough chlorine capacity; E: the curve of CO_2 concentration during the HCl removal process)

Issue 11:

Fig9. The XRD results. Please consider to cut the angle below 10 (Leave too much white space).

Response 11:

Thank you for your comment. Based on reviewer's feedback, we have made modifications to Figure 7, and the revised image is shown below,

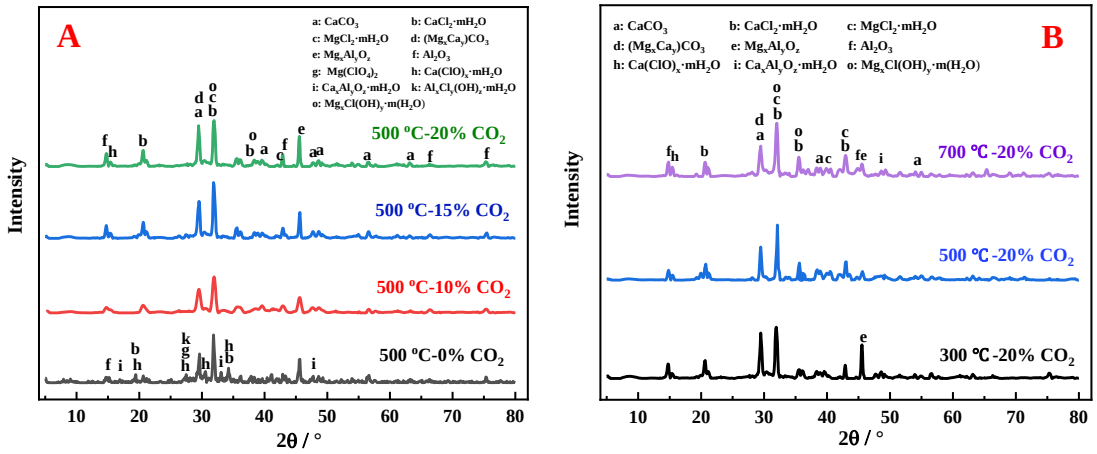

Fig. 9 The XRD patterns of reaction products at different CO_2 concentrations and temperatures (A: the different CO_2 concentrations; B: the different temperatures)

Issue 12:

4 conclusions. Why are the fonts in this section different? The last sentence "These findings align with the proposed reaction mechanism." Is this the key point of the work? It would be better to reach the academic and industrial significance.

Response 12:

Thank you for your comment. Firstly, we apologize for the formatting issue, and we have modified. Secondly, based on your suggestion, we have revised the conclusion, which is as follows,

4. Conclusions

In this study, the performance of HCl removal using Mg-Al-CO_3 and Ca-Mg-Al-CO_3, as modified sorbent, in the presence of CO_2 were investigated.

The Ca-Mg-Al-CO_3 was successfully synthesized with a larger layer spacing d_{003} and particle size compared to Mg-Al-CO_3. CO_2 had a positive impact on the removal of HCl using Mg-Al-CO_3, but a negative impact on the removal of HCl using Ca-Mg-Al-CO_3. However, the performance of HCl removal using Ca-Mg-Al-CO_3 was superior to that of Mg-Al-CO_3. The main reason for this difference is that CO_2 can react with Mg-Al-CO_3 to generate new hydrotalcite intercalated anions through a regeneration process, thereby enhancing the performance of HCl removal. In contrast, Ca-Mg-Al-CO_3 reacted with CO_2 to form large particles of $CaCO_3$, which not only occupied the active sites but also hindered the reaction between HCl and the adsorbent, leading to a decrease in the performance of HCl removal. The main products of reaction between Ca-Mg-Al-CO_3 and HCl were $CaCl_2$ and $MgCl_2$. The presence of CO_2 plays a competitive role in the removal of HCl. The adsorption rate of HCl was initially faster than that of CO_2, but the adsorption capacity of CO_2 was stronger. This can be attributed to the significantly higher concentration of CO_2 compared to HCl. The adsorption reactions of HCl and CO_2 by Ca-Mg-Al-CO_3 was controlled by multiple rate-controlling mechanisms in the early stage of the reaction, and follow a PSO model in the whole process. The study demonstrates that Ca-Mg-Al-CO_3 exhibits excellent performance in removing HCl, which is of significant importance for achieving high-quality synthesis gas and further promoting pyrolysis gasification technology. The findings have academic and industrial significance in advancing waste-to-energy conversion technologies and contributing to the reduction of carbon emissions.

Superscript and subscript.

Response 13:

Thank you for your comment. Based on the reviewer's feedback, we have thoroughly reviewed the superscripts and subscripts, and made the necessary corrections to ensure their accuracy and proper formatting in the revised manuscript.

Highlights

- The performance of Ca-Mg-Al-CO_3 was superior to that of Mg-Al-CO_3 when CO_2 existed
- A competitive relationship between HCl and CO_2 was observed during the adsorption
- The adsorption of HCl and CO_2 followed multiple rate-controlling mechanisms

Effect of CO_2 on HCl removal from syngas using normal and modified Ca-based hydrotalcites: a comparative study

Songshan Cao[1, 2], Jun Cao[3], Hualun Zhu[2], Yaji Huang[1], Baosheng Jin[1]*, Massimiliano Materazzi[2]*

1 Key Laboratory of Energy Thermal Conversion and Control of Ministry of Education, School of Energy and Environment, Southeast University, Nanjing, 210096, China.

2 Department of Chemical Engineering, University College London, London WC1E 7JE, United Kingdom.

3 National Engineering Research Center of Water Resources Efficient Utilization and Engineering Safety, Hohai University, Nanjing 211111, China.

**Corresponding author. Baosheng Jin and Massimiliano Materazzi*

Email: bsjin@seu.edu.cn (Baosheng Jin)

massimiliano.materazzi.09@ucl.ac.uk (Massimiliano Materazzi)

Abstract: MSW pyrolysis and gasification technologies have been recognized as effective means to enhance the resource utilization of MSW and promote a circular economy. However, the presence of HCl gas can significantly impact the quality and application of syngas. To maximize syngas resource utilization, develop highly efficient HCl adsorbent, this study investigates the performance and mechanism of HCl removal from syngas using a conventional hydrotalcite (Mg-Al-CO_3) and modified Ca-based hydrotalcite (Ca-Mg-Al-CO_3). The impact of CO_2, a component naturally presents in syngas, on the performance of both materials, were also investigated. Characterization techniques, including XRD, TGA, SEM, and analysis of pore properties and specific surface area, were employed to understand the underlying reaction mechanism. The results demonstrated that the performance of Ca-Mg-Al-CO_3 was significantly superior to that of conventional Mg-Al-CO_3 sorbents, particularly in the presence of CO_2 However, the presence of CO_2 had a detrimental impact on the performance of Ca-Mg-Al-CO_3 in HCl removal, and this effect became increasingly pronounced with higher concentrations of CO_2. TGA results revealed a

competitive relationship between HCl and CO_2 during the adsorption process. Additionally, the fitting results of adsorption kinetics suggested that the adsorption reaction of HCl and CO_2 by Ca-Mg-Al-CO_3 followed multiple rate-controlling mechanisms.

Keywords: Ca-Mg-Al-CO_3; CO_2; HCl removal; TGA; Adsorption kinetics

1. Introduction

The disposal of municipal solid waste (MSW) has become a pressing issue due to rapid growth of human population and associated industrial activities[1]. The proper utilization of MSW can significantly contribute to the goal of carbon emission reduction[2]. The modern waste management strategies prioritize waste minimization, recycling, and reuse, with landfill disposal considered as the least desirable option to prevent pollution of surface water, groundwater, soil and air, as well as to reduce GHG emissions from the landfill sites. In the background of global carbon neutrality，finding rational ways to utilize MSW is of paramount importance for reducing energy waste and carbon dioxide emissions [3, 4].

The technologies for recovering energy from “residual waste” (i.e., remaining waste that cannot be economically or practically reused or recycled) can play a critical role in mitigating the environmental issues associated to waste disposal. Aside from the valuable product, these technologies can result in a large decrease in the overall amounts of material requiring final disposal. This allows for simpler management in a controlled way while still adhering to pollution control regulations [5]. A host of technologies are available for realizing the potential of residual waste as an energy source (as power or fuel), but the availability and general composition of waste affects the technologies that are suitable to deliver environmental benefits[6]. Thermochemical technologies have historically been used to produce heat and electricity (Waste-to-Energy, or WtE)

via incineration of the waste feedstock, alone or together with other fuels. Most recently, pyrolysis and gasification technologies have been recognized as better methods for achieving higher resource utilization of MSW and circular economy[7]. Compared to traditional treatment methods such as incineration and landfill, pyrolysis and gasification technologies offer several advantages. These technologies not only enable waste disposal while reducing emissions of gaseous pollutants such as NOx and SOx, but also exhibit characteristics such as a small footprint and higher energy efficiencies[8]. Especially in the context of achieving carbon neutrality, the use of pyrolysis and gasification technology for waste processing becomes particularly vital in reducing the pressure of carbon emissions[9, 10]. In the application of the pyrolysis and gasification technology, the gasification technology has a better advantage in resource utilization[11-14]. In the gasification process, as shown in the Fig.1, the combustible solid waste of MSW is introduced into the gasifier. Under a semi-reductive atmosphere, the MSW undergoes thermal decomposition, resulting in the conversion of a substantial portion of the waste into high-value syngas primarily composed of CO, H_2, CO_2 and CH_4 with conversion rates as high as 70% [15]. Additionally, a variable fraction of char or ash is generated. The ash and char residues are transported to specialized factories for comprehensive utilization, including applications such as soil remediation[16] and building materials[17]. The high temperature syngas can directly be utilized in gas turbines or boilers for power generation or heating purposes[18]. Alternatively, it can be directed to industries for the production of high-value by-products[19], showcasing the significant utilization potential of syngas[20, 21].

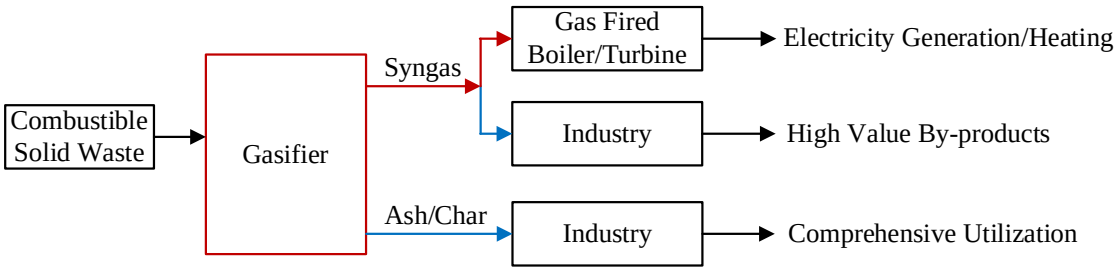

Fig.1 Comprehensive utilization diagram of MSC gasification technology

However, due to the large amount of chlorine-containing substances in MSW[22], those substance are primarily released in the form of HCl gas during gasification process, resulting in the inclusion of significant amounts of HCl gas in the syngas[23]. Consequently, the presence of HCl in syngas can impose limitations and increase application costs. Firstly, the HCl can react with alkali metal, Na and K even at high temperatures, to generate chlorides; these chlorides can cause high temperature corrosion, fouling and slagging of the gasifier and related devices[24, 25]. Secondly, HCl can accelerate migration of heavy metals such as mercury and the formation of dioxins, thereby causing environmental damage and endangering human health[26]. Finally, the high HCl content in syngas results in by-products with high acidity, thereby restricting their quality and application. Those issues pose some serious challenge towards downstream syngas utilization. Therefore, it is necessary to remove HCl prior to application. Currently, conventional methods for HCl removal involve spraying Ca/Na-containing substances into the flue gas or using active carbon to adsorb HCl at low temperatures[27], which have shown favorable results[28-30]. However, these methods have certain disadvantages, particularly when it comes to HCl removal at low temperatures. When applied to remove HCl from syngas, these technologies can result in heat loss in syngas and inefficient heat utilization. Furthermore, the low-temperature HCl removal process can lead to secondary generation of pollutants and partially contaminated waste. Therefore, it is crucial to address these issues by reducing HCl gas using a suitable adsorbent at medium to

high temperatures (300 – 700 ºC). This step is essential for enhancing the quality of syngas and enabling further applications.

Hydrotalcite is a kind of metal oxide compound with a layered porous structure and double hydroxyl groups, which exhibits acid-base bifunctionality and thermal stability. Since its discovery, it has been extensively used as adsorbent, catalyst and catalyst carrier[31-33]. Researchers have also explored the modification of hydrotalcite by incorporating metals with different properties, resulting in hydrotalcite-like compound. These modified hydrotalcite materials demonstrate enhanced performances to satisfy the specific application requirements[34, 35]. Hydrotalcite and hydrotalcite-like compounds have demonstrated effective adsorption performance for Cl^- in an aqueous environment [36, 37], as well as HCl from flue gases[38, 39]. Previous studies have specifically investigated the effects of hydrotalcite preparation conditions and operating parameters on the performance of HCl removal using simplified HCl gas simulations on the performance of HCl removal suing simulated HCl gas atmospheres[40]. In these studies, it was observed that the hydrotalcite-like compound modified with Ca^{2+} (Ca-Mg-Al-CO_3) exhibited superior HCl removal performance. Additionally, Ca-Mg-Al-CO_3 can be utilized at higher temperatures[41]. Therefore, in this current study, we chosen Ca-based nitrate to modify Mg-Al-CO_3, and both Ca-Mg-Al-CO_3 and Mg-Al-CO_3 were selected to remove HCl as a comparison. It is important to note that CO_2, a non-combustible gas, is present in syngas at significantly higher concentrations than HCl. CO_2 is a key component in various processes, including the water-gas shift reaction, producing CO and so on , It has been established that hydrotalcite can adsorb CO_2 effectively.[42, 43] CO_2 is also confirmed to be adsorbed by hydrotalcite [44, 45]. Therefore, both HCl and CO_2 can be adsorbed by hydrotalcite. Especially in the case of Ca-Mg-Al-CO_3, it exhibits

remarkable capabilities in adsorbing CO_2 due to the generation of calcium-containing oxide at mid-high temperatures[46, 47]. Consequently, the presence of CO_2 may influence the performance of HCl removal using hydrotalcite and Ca-Mg-Al-CO_3, although the specific effect tendency is not yet well understood. Although some studies have reported on the effect of CO_2 on HCl removal using other calcium-based compounds such as CaO, $Ca(OH)_2$ and $CaCO_3$[48, 49], it should be noted that the research objectives and operating conditions varied, resulting in inconsistent results. Therefore, when studying the performance of HCl removal in syngas, the effect of CO_2 on HCl removal using hydrotalcite and hydrotalcite-like compounds should not be overlooked. Surprisingly, there is a lack of research focusing on the characteristics of HCl removal using hydrotalcite and hydrotalcite-like compound in the presence of CO_2. Therefore, it is necessary to analyze the effect and mechanism of CO_2 on HCl removal by adsorbent. Obtaining the impact tendency of CO_2 on HCl removal by hydrotalcite is crucial for ensuring the production of high-quality syngas and expanding the applications of syngas in various fields.

To obtain high-performance adsorbents and maximize syngas resource utilization, this study focuses on the utilization of Mg-Al-CO_3 and modified Ca-based hydrotalcite-like (Ca-Mg-Al-CO_3) for HCl removal at mid-high temperatures, to analyze of the effect of Ca^{2+} modification on the HCl removal performance of hydrotalcite Firstly, the Mg-Al-CO_3 and Ca-Mg-Al-CO_3 were synthesized using the coprecipitation method. Subsequently, the impact of CO_2 on HCl removal by Mg-Al-CO_3 and Ca-Mg-Al-CO_3 was investigated under different conditions, with a comparative analysis. To further understand the adsorption relationship of CO_2 and HCl by Ca-Mg-Al-CO_3, thermogravimetric analysis (TGA) was employed. The characterization instruments of XRD and the specific surface area and pore size were used to analysis the reaction mechanism. Finally, the

adsorption kinetics were chosen to investigate the adsorption mechanism of HCl removal using Ca-Mg-Al-CO_3 in the presence of CO_2.

2. Material and Methods

2.1 Synthetic steps

In this study, the chemical reagents of Mg $(NO_3)_2 \cdot 6H_2O$, Al $(NO_3)_3 \cdot 9H_2O$, Ca $(NO_3)_2 \cdot 4H_2O$, NaOH and Na_2CO_3 with analytically pure grade were produced from Sinopharm Chemical Reagent Co., Ltd. The Mg-Al hydrotalcite containing CO_3^{2-} intercalated (Mg-Al-CO_3), and Ca-based modified hydrotalcite-like (Ca-Mg-Al-CO_3) were synthesized using the coprecipitation method for gaseous HCl removal. The synthetic process is shown in Fig. 2 and the synthetic steps are as follows.

Preparation of Mg-Al-CO_3: (1) According to the molar ratio of Mg/Al=3, $[OH^-]=2([Mg^{2+}]+[Al^{3+}])$ and $[CO_3^{2-}] =1/2[Al^{3+}]$, the corresponding chemical reagents were weighed. (2) The nitrates and two bases were dissolved in ultra-pure water at 60 °C, respectively. (3) The two solutions were dropped into a four-port flask at a certain speed using a peristaltic pump at 60 °C. During this process, the pH value was maintained at 11, and the stirring speed was set at 300 r/min. The resulting mixture was continuously stirred for 2 hours at 60 °C. (4) The obtained substance was subjected to crystal growth for 20 hours at 80 °C. (5) The solid part was washed using ultra-pure water until neutral, dried and grounded. The Mg-Al-CO_3 was obtained, and the particles in size range of 40 to 60 mesh were chosen for subsequent experiments.

Preparation of Ca-Mg-Al-CO_3: The Ca-Mg-Al-CO_3 was prepared with a molar ratio of $Ca^{2+}/Mg^{2+}= (Ca+Mg)^{2+}/Al^{3+}=3$, $[OH^-]=2([(Ca+Mg)^{2+}] + [Al^{3+}])$ and $2[CO_3^{2-}] = [Al^{3+}]$. The step (2) to (5) mentioned above were repeated to obtain Ca-Mg-Al-CO_3, and the particle sizes range was the same as that of Mg-Al-CO_3.

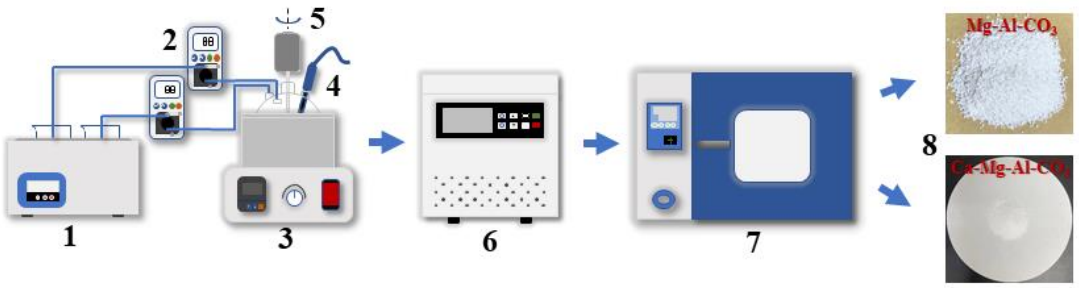

1. Thermostatic water pot; 2. Peristaltic pump; 3 Thermostatic oil pot; 4. pH meter; 5. Mixer; 6. Centrifuge; 7. Drying oven; 8. Adsorbents

Fig. 2 Synthetic process of adsorbents

2.2 Characterization

X-ray diffraction（XRD）analysis was made using the Bruker D8 ADVANCE equipment by Bruker Daltonics Inc., Germany. The diffraction angle range was set from 5 to 80 ° with a step size of 0.08 °. The equipment model of scanning electron microscope (SEM) was S4800 from Hitachi Limited. Energy Dispersive Spectroscopy (EDS) equipment from EDAX. Inc was employed for elemental analysis. The specific surface area and pore size analyzer (ASAP 2460, Micromeritics Instruments Corporation, America) was used to analyze the specific surface area and pore structure of adsorbents. Thermogravimetric analysis (TGA) for thermal stability analysis was carried out using the (PerkinElmer TA 8000) produced by platinum Elmer Co., Ltd.

2.3 Experimental equipment and steps

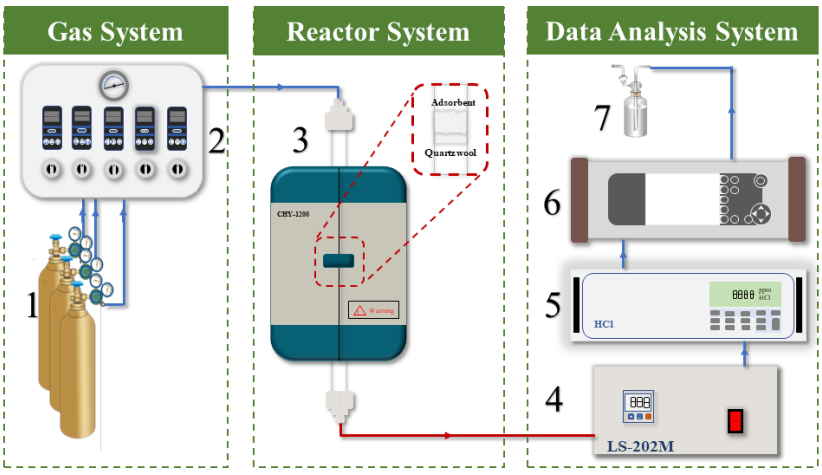

1. Gas cylinder; 2. Mass flowmeter; 3. Reactor; 4. LJ-202M condenser; 5. HCl analyzer; 6. Flue

gas analyzer; 7. Gas-washing bottle

A. The schematic diagram of experiments

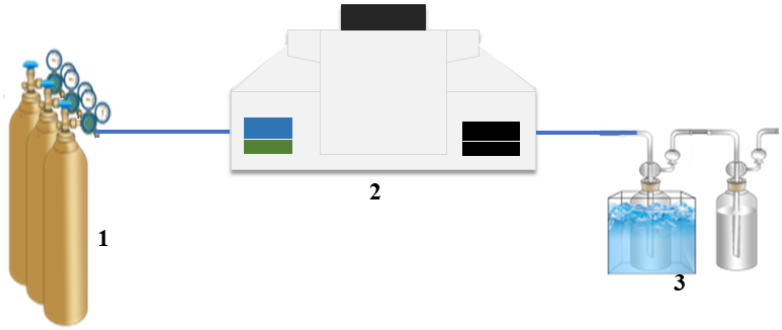

1. Gas cylinder; 2. Thermogravimetric analyzer; 3. Gas-washing bottle

B. Experimental schematic diagram of thermogravimetry analysis (TGA)

Fig.3 Experimental schematic diagram

The HCl (Signal Group Ltd., UK) and the CO_2 (MRU Instruments, Inc., Germany) analyzers warmed up and calibrated. Before conducting experiments, a blank test was performed involving both CO_2 and HCl to ensure that there was no mutual interference. Then the absorbent was placed in the middle of the reactor, the reactor temperature was gradually increased to desired reaction temperature at a heating rate of 10 ^oC/min in a N_2 atmosphere. Once the reaction temperature reached a steady state, a mixture of N_2, HCl and CO_2 in specific proportions was introduced into the reactor using mass flowmeters. Simultaneously, the analyzers started monitoring the gas composition. To prevent the release of HCl and CO_2 into the environment, an aqueous solution of 0.3 mol/L NaOH was used to adsorb the excess HCl and CO_2. The specific operating conditions of the experiments are listed in Table.1. High-purity N_2 and CO_2 with a grade of 99.999 % grade and HCl concentration of 2000 ppmv from Nanjing Special Gas Plant Co., Ltd. were employed in the tests.

Table. 1 The operating conditions of tests

Parameters	Unit	HCl Removal	TGA
Material	/	Mg-Al-CO_3, Ca-Mg-Al-CO_3	Ca-Mg-Al-CO_3
Reaction temperature	^oC	300, 400, 500, 600, 700	500
HCl concentration	ppmv	400	400
CO_2 concentration	vol. %	0, 10, 15, 20, 25	20

Quality	mg	500	20
Gas flow	L/min	0.5	0.1
Reaction time	h	/	5
Particle diameter	nm	0.25-0.38	
Gas	/	HCl, N_2, CO_2	

190

191 **2.4 Experimental data processing**

192 The instantaneous HCl removal rate is calculated by Eq. 1.

193 $$\eta = \frac{C_{in} - C_{out}}{C_{in}} \times 100\% \quad \text{Eq. 1}$$

194 The HCl average removal rate is calculated by Eq. 2.

195 $$\overline{\eta} = \frac{1}{N}\sum_{i=1}^{N} \eta_i \quad \text{Eq. 2}$$

196 The breakthrough chlorine capacity refers to the total mass of HCl adsorbed per unit mass of
197 adsorbent from the start of the reaction until complete breakthrough occurs. The breakthrough
198 chlorine capacity is calculated by Eq. 3[50].

199 $$Q_t = 10^{-3}\int_0^t \frac{36.5(C_0 - C_{out})V_s}{22.4m}dt \quad \text{Eq. 3}$$

200 Where η and η_i, $\overline{\eta}$ are instantaneous HCl removal rate, HCl removal rate at t time and HCl
201 average removal rate, %, i=1, 2, 3, …, N. C_0, C_{in} and C_{out} are HCl concentration of initial, inlet,
202 and outlet, ppmv. Q_t is the saturation chlorine content, mg/g. V_s is volume flow of reaction gas,
203 L/min. m is the quality of adsorbent, g.

204 The Intra-particle diffusion model is commonly used to assess whether diffusion is the sole rate-
205 controlling step in a reaction. The equation is given by Eq. 4[51].

206 $$q_t = k_1 t^{1/2} + C \quad \text{Eq. 4}$$

207 Where q_t is the adsorption capacity of adsorbent at time t, mg·g^{-1}. k_1 is the rate constant of
208 intragranular diffusion model, mg· (g·min$^{-1/2}$)$^{-1}$. C is constant, mg·g^{-1}.

209 The pseudo-first-order model (PFO) is employed to determine whether the adsorption process is
210 controlled by diffusion or surface reaction, when adsorption is controlled by chemical adsorption
211 of chemical factors, the equation is described by Eq. 5[52].

$$\log(q_e - q_t) = \log q_e - \log(\frac{k_1}{2.303}) \quad \text{Eq. 5}$$

Where q_e represents HCl equilibrium adsorption amount, mg·g^{-1}. q_t is the HCl adsorption capacity at time t. k_1 is the rate constant, min^{-1}.

The pseudo-second-order (PSO) model is predicated on the assumption that the adsorption rate is controlled by a chemical adsorption mechanism, involving electron sharing or electron transfer between the adsorbent and the adsorbate. The equation for this model is represented as Eq. 6[53].

$$\frac{t}{q_t} = \frac{1}{k_2 q_e^2} + \frac{1}{q_e} \quad \text{Eq. 6}$$

Where q_e represents HCl equilibrium adsorption capacity, mg·g^{-1}. q_t is the HCl adsorption capacity at time t. k_2 is the rate constant, min^{-1}.

The Elovich model is indeed a commonly used model for describing the chemical adsorption of gases on solid surfaces. The Elovich model is defined as Eq.7[54].

$$q_t = (\frac{2.3}{k_0})\lg(t + t_0) - (\frac{2.3}{k_0})\lg t_0 \quad \text{Eq. 7}$$

Where $t_0 = 1/k_0 k_f$. k_0 is initial adsorption rate at q_t = 0, mg /g·min. k_f is desorption constant, g·mg. Eq. 7 is simplified with $tk_0k_f << 1$, t=0, q_t=0.

$$q_t = k_0 \ln(k_f k_0) + k_0 \ln(t) \quad \text{Eq. 8}$$

The Bangham model is used to describe pore diffusion, which optimizes Lagergren model through time compensation, so that it has been well applied in predicting the adsorption process of various adsorbents. The model function is shown in Eq. 9[55].

$$\lg\{\lg[q_e / (q_{e-} q_t)]\} = \lg(\frac{k_2}{2.303}) + n\lg t \quad \text{Eq. 9}$$

Where q_t is adsorption capacity of adsorbent at time t, mg·g^{-1}. q_e is HCl equilibrium adsorption capacity, g·min. k_1 is rate constant of intragranular diffusion model, mg· (g·min$^{-1/2}$)$^{-1}$. C is constant, mg·g^{-1}. k_2 is the Bangham rate constant.

3. Results and Discussion

3.1 Characterization of adsorbents

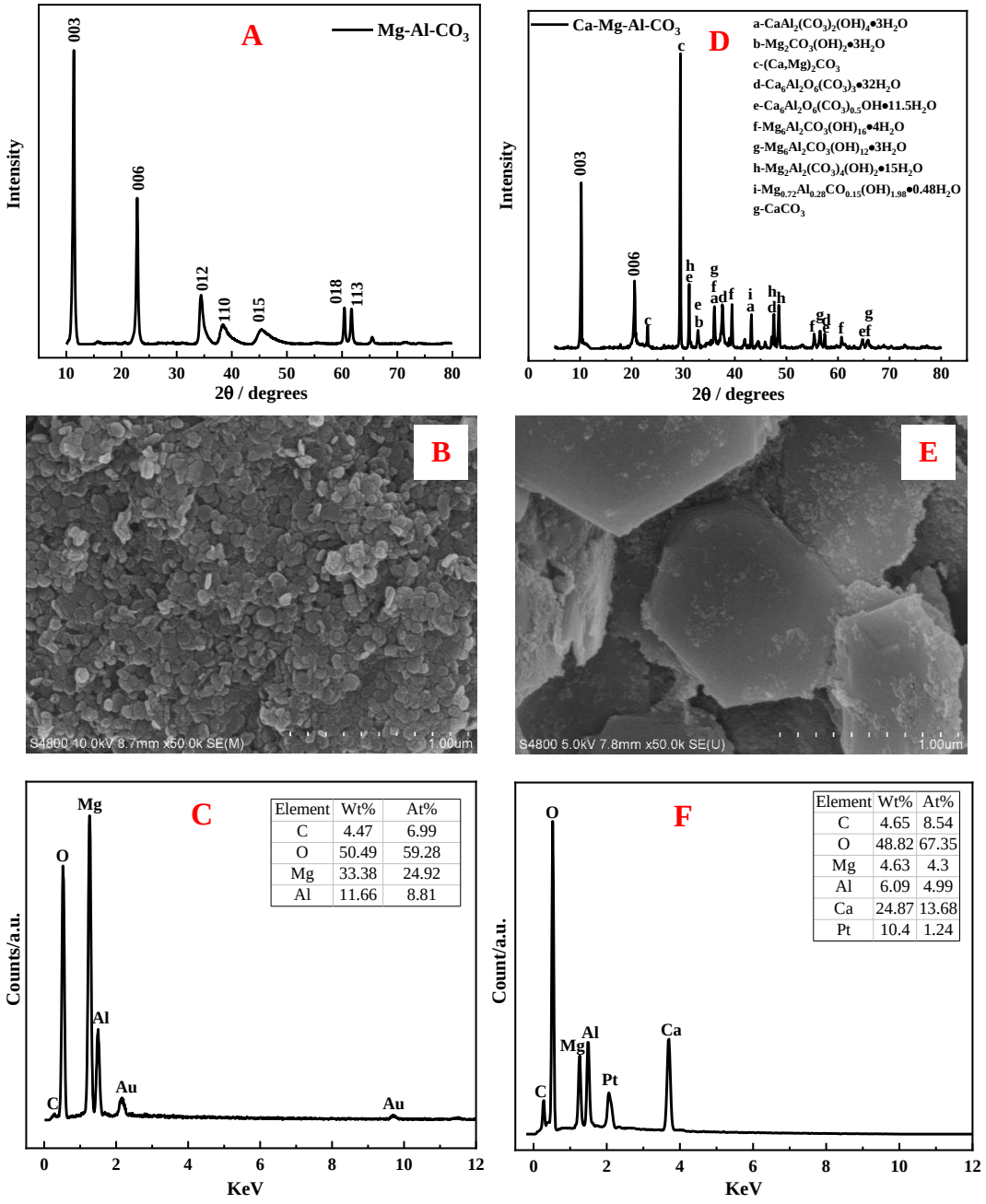

Fig. 4 Characterization of adsorbents (Mg-Al-CO_3: A: XRD pattern, B: SEM image, C: EDS pattern; Ca-Mg-Al-CO_3: D: XRD pattern, E: SEM image, F: EDS pattern)

The characterization results of Mg-Al-CO_3 and Ca-Mg-Al-CO_3 are presented in Fig. 4. From Fig.4 A, B and C, it can be observed that the molar ratio of Mg/Al was 2.8, the characteristic diffraction peaks of hydrotalcite (PDF-＃35-0965) were evident in Mg-Al-CO_3, including crystal faces of hydrotalcite such as (003), (006), (012), (015), (018), (110), and (113). The layer spacing

of d_{003} of Mg-Al-CO_3 was determined to be 0.78 nm. The SEM image revealed that Mg-Al-CO_3 exhibited a regular hexagonal lamellar structure, the width and thickness of layered Mg-Al-CO_3 were approximately around 400 nm and 50nm, respectively. Fig. 4 D, E, and F present the XRD pattern, SEM image and EDS pattern of Ca-Mg-Al-CO_3, respectively. Ca-Mg-Al-CO_3 showed obvious characteristic diffraction peaks of (003) and (006) with a narrow peak pattern and high intensity, the layer spacing of d_{003} in Ca-Mg-Al-CO_3 was 1.02 nm. The SEM image in Fig. 4E confirmed the presence of a hexagonal lamellar structure in Ca-Mg-Al-CO_3. The molar rate of Ca/Mg was determined to be 3.18, and the ratio of $(Ca+Mg)^{2+}$/ Al^{3+} was 3.6. These results indicate the successful synthesis of the layered structure of Mg-Al-CO_3 and Ca-Mg-Al-CO_3. A comparison between the characterization results of Mg-Al-CO_3 and Ca-Mg-Al-CO_3 suggests that the prepared Mg-Al-CO_3 exhibits a single crystal phase with good crystallinity. The structure size of Ca-Mg-Al-CO_3 was larger than that of Mg-Al-CO_3 from Fig. B and E. However, Ca-Mg-Al-CO_3 had some impurities, as evidenced by the presence of characteristic peaks corresponding to $CaCO_3$ found in the XRD pattern, this suggests the occurrence of a small amount of $CaCO_3$ impurities in Ca-Mg-Al-CO_3. The main reason for this phenomenon can be attributed to the difference in ion radius that the ion radius of Ca^{2+}, $Mg^{2+}$and Al^{3+} are 0.100nm, 0.072nm and 0.0535nm, respectively, the ion radius of Ca^{2+} is larger than that of Mg^{2+} and Al^{3+}. The presence of Ca^{2+} as a substitute for some Mg^{2+} in the formation of Ca-Mg-Al-CO_3 resulted in incompatibility, leading to the formation of $CaCO_3$. Additionally, the low solubility product constant of $CaCO_3$ contributed to its formation during the preparation of Ca-Mg-Al-CO_3. These results showed that the structure of hydrotalcite can be modified by the addition of Ca^{2+}, resulting in changes in its characteristics and the formation of $CaCO_3$ impurities.

3.2 The performance of HCl removal by Mg-Al-CO_3

3.2.1 The effect of CO_2 concentration on HCl removal

When there is HCl gas in the outlet gas, the corresponding point on the breakthrough curve is referred to as the breakthrough point, and the time at this point is known as the breakthrough time. In Fig.5, the breakthrough curve, average HCl removal rate, and adsorption chlorine capacity of Mg-Al-CO_3 are displayed for an HCl concentration of 400 ppmv, a flow rate of 500 mL/min, a reaction temperature of 300 ℃, and CO_2 concentrations ranging from 0 to 25%. As shown in Fig. 5A, the breakthrough curves initially shift towards left and then towards the right with increasing CO_2 concentration. The Mg-Al-CO_3 adsorbent exhibits the highest adsorption capacity when the CO_2 concentration is at 15 % during a period of 300 min. The breakthrough time increased from approximately 17 min to 115 min, and then decreased from approximately 115 min to 73 min. Compared to the adsorption effect without CO_2, the adsorption capacity has increased by at least 329.4% with the presence of CO_2, indicating that CO_2 has a positive effect on improving the adsorption capacity of Mg-Al-CO_3. The average HCl removal rates are presented in Fig 5B. It can be observed that the average HCl removal rates decreased rapidly with the increase of reaction time. When the CO_2 concentration rises from 0 to 15%, the average HCl removal rate increased from 85.2 % to 100 % when the CO_2 concentration increased from 0 to 15 %, showing an increase of 17.4%. Subsequently, it decreased from 100 % to 97.2 % over a period of 100 mins. As the reaction time extended from 100 to 500 mins, the HCl removal rates decreased by 67.6 %, 51.8 %, 40 %, 51.7 %, and 54.6 %, respectively, as the CO_2 concentration increased from 0 to 25 %. Comparing the HCl removal effect with and without CO_2, it can be concluded that the performance of HCl removal was enhanced when the simulation gas contained CO_2. This main

reason for this improvement is that hydrotalcite exhibits a memory function, enabling it to regenerate under appropriate conditions when the structure is not completely destroyed[50], this process was employed as depicted in *React. 1*. Therefore, the structure of Mg-Al-CO_3 undergoes regeneration when CO_2 participated in the reaction at 300 ℃. $Mg_{3n}Al_nO_{9n/2}$, which was difficult to react with HCl, participated in the reaction again, resulting in the addition of the active sites on the surface of the adsorbent. The structure regeneration of Mg-Al-CO_3 leads to the replacement of more CO_3^{2-} for Cl^-, and further enhancing HCl removal performance of the adsorbents. Consequently, the effect of HCl removal increases with the increase of CO_2 concentration. And the regeneration process was optimal with 15% CO_2.

$$Mg_{3n}Al_nO_{9n/2} + (n/2)\ CO_2 + (m+4n)\ H_2O \rightleftharpoons Mg_{3n}Al_n(OH)_{8n}(CO_3)_{n/2} \bullet mH_2O \quad (React.\ 1)$$

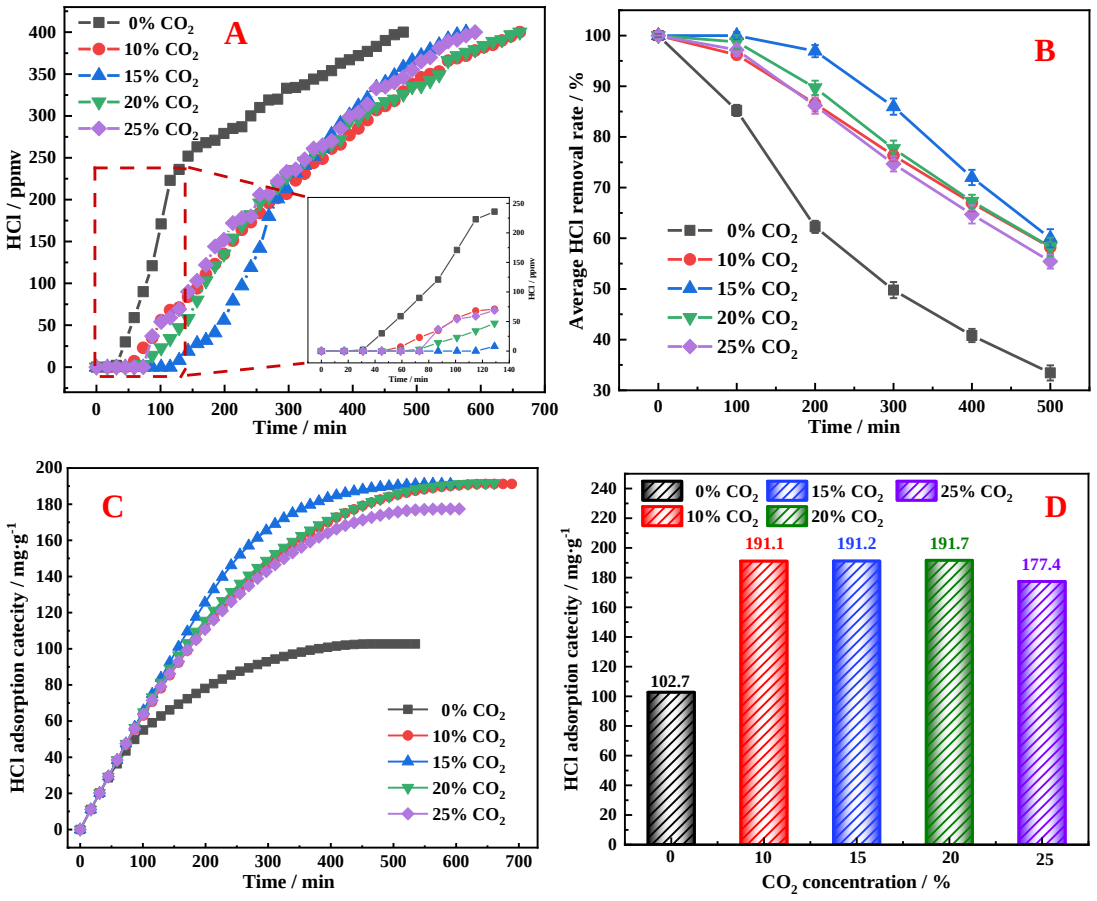

Fig. 5 The performance of HCl removal using Mg-Al-CO_3 at different CO_2 concentrations (A: the

breakthrough curves; B: the average HCl removal rate; C: the adsorption chlorine capacity curves; D: the maximum breakthrough chlorine capacity)

The chlorine adsorption capacity curves and the breakthrough chlorine capacity of Mg-Al-CO_3 are shown in Fig. 5C and D. In the presence of CO_2 (Fig. 5C), Mg-Al-CO_3 exhibited significantly higher chlorine adsorption capacity compared to the absence of CO_2. Additionally, Fig.5 D indicates an increase in the breakthrough chlorine capacity of approximately 86 % - 87 % with CO_2 concentrations ranging from 10 %-20 %, stabilizing at around 191 $mg \cdot g^{-1}$. However, beyond a CO_2 concentration of 20%, the breakthrough chlorine capacity started to decrease, indicating a decline in the HCl removal performance of Mg-Al-CO_3. This decline can be attributed to the high CO_2 content, which increased the diffusion resistance of HCl, impeding its reaction with the adsorbent.

3.2.2 The effect of reaction temperature on HCl removal

The breakthrough curves, average HCl removal rates and the adsorption chlorine capacity of Mg-Al-CO_3 are depicted in Fig. 6. The experiments were conducted at an HCl concentration of 400 ppmv, a flow rate of 500 mL/min, a CO_2 concentration of 20 %, and a reaction temperature ranging from 300 to 700 ℃ with intervals of 100 ℃. In Fig. 6A, as the temperature increased, the breakthrough curves shifted to left, indicating a decrease in the effective HCl adsorption time from 650 min to 130min. The breakthrough time initially increased from 59 min to 73 min as the reaction temperature increased from 300 to 500 ℃, but then decreased from 73 min to 31 min. The adsorption capacities at 400 ℃ and 500 ℃ were better than that at 300 ℃, occurring at around 170 min and 100 min, respectively. The optimal performance of HCl removal using Mg-Al-CO_3 was observed at 400 ℃ within the first 200 min. However, although the adsorption capacity

increased within the first 200 min at 400 ℃, the rate of HCl adsorption showed a declining trend. The average HCl removal rates of Mg-Al-CO_3 are presented in Fig. 6B, the average HCl removal rates of Mg-Al-CO_3 at 400 and 500 ℃ were higher than that at 300 ℃ in the first 100 min, and the average HCl removal rate of Mg-Al-CO_3 at 400 ℃ surpassed that at 300 ℃ within the first 200 min, reaching 90.7%. This improvement can be attributed to the creation of the new porous structure resulting from the release of moisture and CO_2 during the thermal decompaction of Mg-Al-CO_3[31]. The abundant pore structure can provide more active sites, facilitating the reaction between the absorbent with HCl. With the increase in reaction temperature, the pore structure becomes more pronounced. However, as the reaction temperature exceeded the pore structure of Mg-Al-CO_3 was disrupted, leading to the formation of spinel and a loss of regenerative capacity. The magnesium aluminum oxide generated in high-temperature was not conducive to the reaction of HCl removal. Consequently, the HCl adsorption capacity decreased and the HCl removal rates diminished when the reaction temperature surpassed 400 ℃.

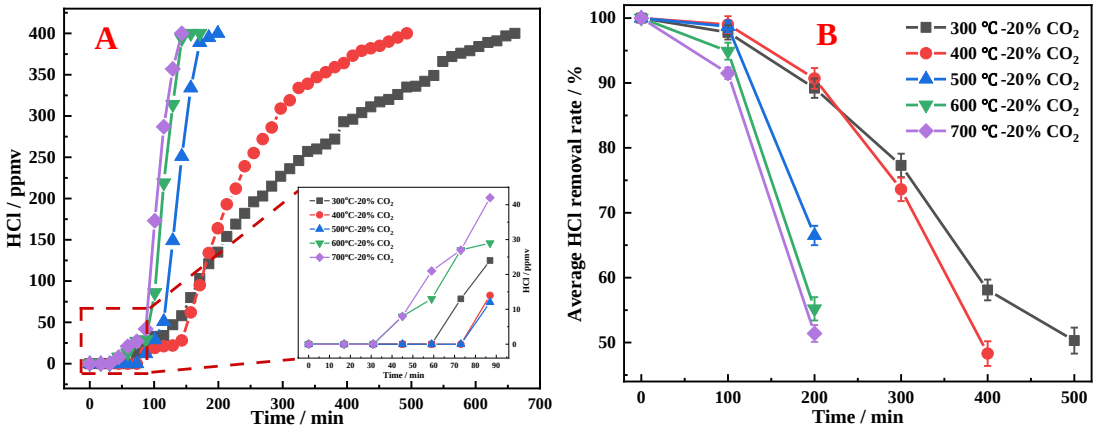

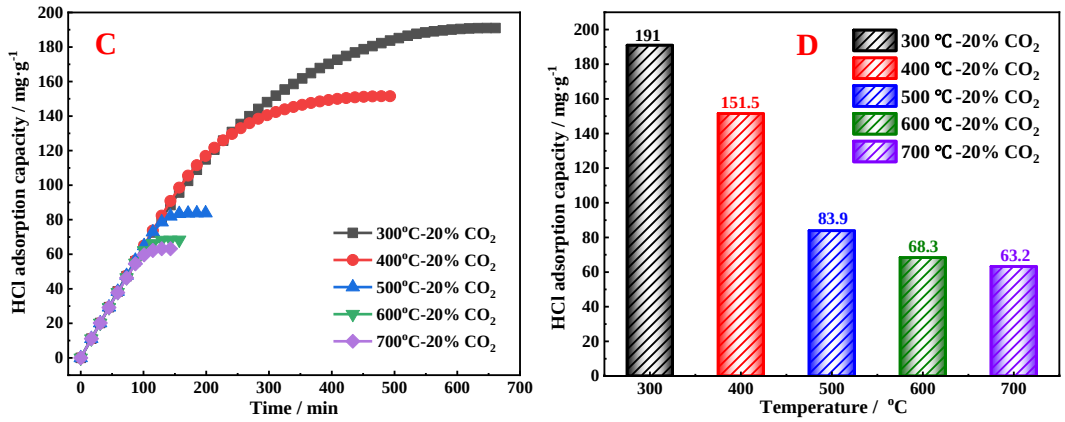

Fig. 6 The performance of HCl removal using Mg-Al-CO_3 at different temperatures (A: the breakthrough curves; B: the average HCl removal rate; C: the adsorption chlorine capacity curves; D: the maximum breakthrough chlorine capacity)

In Fig. 6C, the adsorption chlorine capacity of Mg-Al-CO_3 exhibits trends consistent with the breakthrough curves. Fig. 6B shows the HCl removal rates, which demonstrated good performance at 400 ℃ in first 200 min. However, the chlorine adsorption capacity decreased from 191 to 63.2 $mg \cdot g^{-1}$ as the reaction temperature increased from 300 to 700℃, resulting in a decrease of 66.9 %. This reduction can be attributed to the decrease in effective reactive substances as the reaction temperature increased. These results indicate that while CO_2 enhanced the HCl removal performance of Mg-Al-CO_3, temperature played a more significant role in determining the HCl removal performance of Mg-Al-CO_3. Additionally, and the complete structure of hydrotalcite also contributed to the favorable HCl removal capacity.

3.3 The performance of HCl removal by Ca-Mg-Al-CO_3

3.3.1 The effect of CO_2 concentration on HCl removal performance

The effects of different CO_2 concentrations on HCl removal by Ca-Mg-Al-CO_3 were investigated, and the results are presented in Fig. 7 A-D. The experiments were conducted at a temperature of 300 ℃, HCl concentration of 400 ppmv and CO_2 concentrations ranging from 0 to

25 %. The breakthrough curves of HCl adsorption by Ca-Mg-Al-CO_3 are shown in Fig.7A. The reaction time of HCl removal by Ca-Mg-Al-CO_3 was 3 times that of Mg-Al-CO_3 without CO_2. It can be observed that the reaction time decreased from 1430 min to 783 min with the increase of CO_2 concentrations from 0 to 25 %, decreased by 45.24 %, indicating that the adsorption capacities of Ca-Mg-Al-CO_3 decreased with the increase of CO_2 concentration. Compared to the optimal HCl removal performance of Mg-Al-CO_3, the reaction time increased by more than 2 times. When CO_2 concentrations rose from 10 to 25 %, the adsorption time only decreased by 9.64 %, suggesting a minor impact on HCl removal by Ca-Mg-Al-CO_3 with a continuous increase of CO_2 concentration. The breakthrough time also decreased from approximately 60 min to 45 min, representing a decrease of 25 %. In Fig. 7B, the average HCl removal rates exhibited a decreasing trend with the presence of CO_2. Compared to the reaction without CO_2, the reduction in average HCl removal rates was more pronounced in the presence of CO_2 after 100 min. The average HCl rates of adsorbent at 0 % and 25 % CO_2 were 98.2 % and 95.7 %, respectively, at 100 min, indicating a decrease of only 2.5 %. However, a decrease of 11 % was observed at 500 min. The phenomenon demonstrates that the presence of CO_2 has a negative effect on HCl removal, and this effect becomes increasingly evident with higher CO_2 concentration.

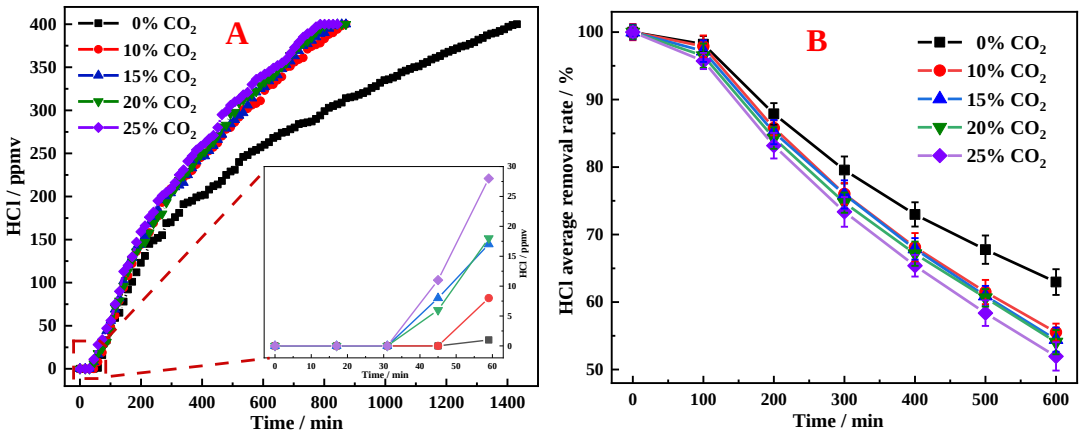

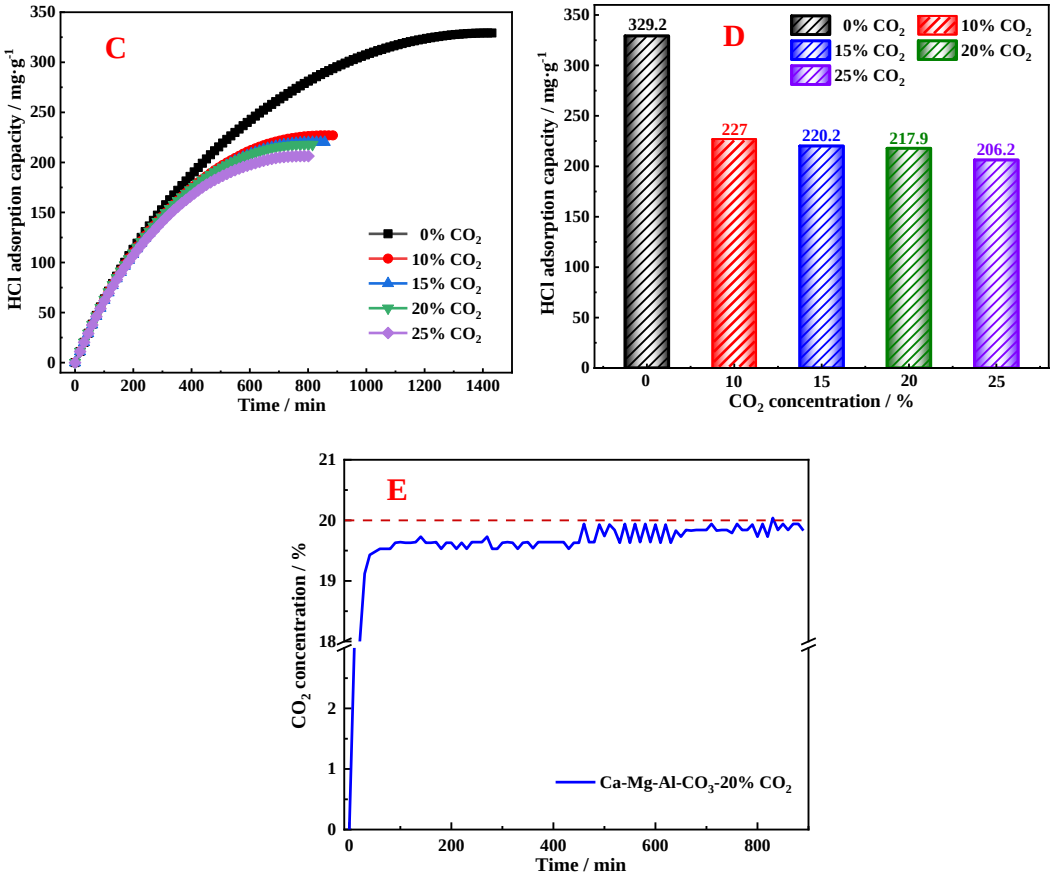

373

374

375 Fig.7 The performance of HCl removal using Ca-Mg-Al-CO_3 under different CO_2 concentrations

376 and the change curve of CO_2 (A: the breakthrough curves; B: the average removal of HCl rate; C:

377 the adsorption chlorine capacity curves; D: the maximum breakthrough chlorine capacity; E: the

378 curve of CO_2 concentration during the HCl removal process)

379 Fig. 7C illustrates the breakthrough chlorine capacity of Ca-Mg-Al-CO_3 at different CO_2

380 concentrations. It is evident from the figure that as the CO_2 concentration, the breakthrough

381 chlorine capacity decreased rapidly. This trend is further supported by Fig. 7D, which

382 demonstrates that the maximum breakthrough chlorine capacity of Ca-Mg-Al-CO_3 decreased from

383 329.2 mg/g to 227 mg/g when the CO_2 concentrations increased from 0 to 10 %, representing a

384 decrease of 37.4 %. However, the decrease was only 6.4 % when the CO_2 concentration increased

385 from 10 to 25 %. Fig. 7E shows the change in CO_2 concentration during the removal of HCl,

specifically focusing on the curve for 20 % CO_2. It is can be seen that the concentration of CO_2 exhibited a slow increase with increasing reaction time, indicating that CO_2 can also be adsorbed by Ca-Mg-Al-CO_3. Especially within 450 min, the concentration of CO_2 remained around 19.65 %. The result implied that CO_2 also could be adsorbed by Ca-Mg-Al-$CO_3$and reacted with partly Ca-oxide to generate $CaCO_3$. The presence of $CaCO_3$ reduced the adsorption activity of HCl, thereby decreasing the performance of HCl removal. Despite the negative impact of CO_2 on the performance of HCl removal by Ca-Mg-Al-CO_3, it is noteworthy that the overall performance of Ca-Mg-Al-CO_3 was better than that of Mg-Al-CO_3.

3.3.2 The effect of reaction temperature on HCl removal performance

In Fig. 8, the change curves depict the effect of different reaction temperatures on the HCl removal performance of Ca-Mg-Al-CO_3. The experimental conditions included a CO_2 concentration of 20 %, an initial HCl concentration of 400 ppmv, and reaction temperatures ranging from 300 to 700 ℃ in intervals of 100 ℃. As shown in Fig.8A, the breakthrough curves shifted to the left first and then to the right with the increase of reaction temperature, the optimal HCl adsorption performance of HCl adsorption was observed at 500 ℃, with a breakthrough time of approximately 190 min. This represented a significant increase of 496.8 % compared to the optimal performance of Mg-Al-CO_3. When reaction temperature increased from 300 ºC to 500 ºC, the reaction time increased from 801min to 1123min, indicating an increase of 28.67 %. However, as the temperature further increased from 500 to 700 ºC, the reaction time decreased from 1123 min to 857 min, representing a decrease of 23.69%. Fig. 8B illustrates the change tendencies of average HCl removal rates, which aligned with the patterns observed in the breakthrough curves. The best HCl removal performance was achieved at 500 ℃, with an average HCl removal rate

exceeding 80 % within 600 min.

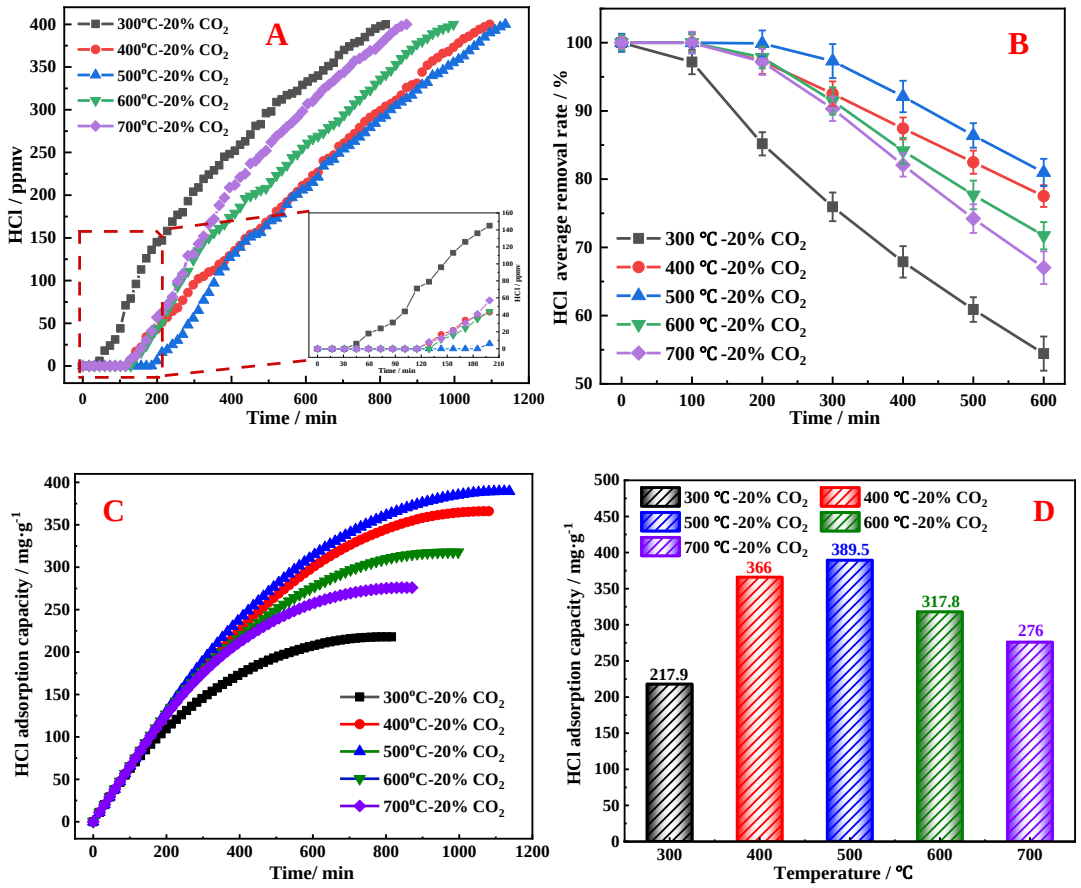

Fig. 8 The performance of HCl removal using Ca-Mg-Al-CO_3 at different CO_2 atmosphere (A: the breakthrough curves; B: the average removal of HCl rate; C: the adsorption chlorine capacity curves; D: the maximum breakthrough chlorine capacity)

Fig. 8C presents the change curves of the adsorption chlorine capacity at different temperatures. The adsorption chlorine capacities exhibited an initial increase followed by a decrease as the reaction temperature was raised. This behavior is further supported by Fig.8 D, which indicates that the maximum breakthrough chlorine capacity of Ca-Mg-Al-CO_3 increased from 217.9 mg/g to 389.5 mg/g as the reaction temperature increased from 300 to 500 ℃, then decreased from 389.5 mg/g to 276 mg/g as the reaction temperature further increased from 500 to 700 ℃. These findings emphasize the significant influence of reaction temperature on the HCl removal performance of

Ca-Mg-Al-CO_3 under CO_2 atmosphere, with the optimal performance observed at 500 ℃, reaching 389.5 mg/g.

The observed results can be attributed to several factors. Firstly, the increase in reaction temperature promotes the development of the pore structure in Ca-Mg-Al-CO_3, leading to a larger specific surface area and an increase in the number of basic active sites. These changes enhance the adsorption and reaction of HCl with the adsorbent. The presence of Ca^{2+} in the hydrotalcite structure plays a crucial role in determining the optimal condition at 500 ℃. At this temperature, the Ca-Mg-Al-CO_3 exhibits the highest performance in HCl removal. However, when the temperature exceeds 500 ℃, the porous structure of the hydrotalcite can be destroyed, the effective component of HCl removal decreased and more substances that were not easy to react with HCl were generated (such as spinel). These transformations prevent the regeneration of the hydrotalcite structure and lead to a decrease in the number of active sites on the surface. Consequently, the reaction paths involving Cl^- replacing CO_3^{2-} and the reaction of Cl^- with Ca^{2+} are hindered, resulting in a reduction in the performance of HCl removal. Therefore, the optimal temperature for efficient HCl removal by Ca-Mg-Al-CO_3 was determined to be 500 ℃, while temperatures above this threshold were detrimental to the adsorption capacity and overall performance.

The results of the HCl removal using Mg-Al-CO_3 and Ca-Mg-Al-CO_3 in the presence of CO_2 indicate different effects of CO_2 on their performance. In the case of Mg-Al-CO_3, CO_2 has a positive impact on HCl removal, whereas in the case of Ca-Mg-Al-CO_3, CO_2 has a negative effect. Despite the adverse effect of CO_2 on Ca-Mg-Al-CO_3, the overall performance of HCl removal using Ca-Mg-Al-CO_3 was better than that of Mg-Al-CO_3. When the Mg-Al-CO_3 was modified by introducing Ca^{2+}, the optimum reaction temperature was 500 ℃, and the maximum breakthrough

chlorine capacity increased to 389.5 mg/g, representing a 103.7 % increase compared to the highest breakthrough chlorine capacity of Mg-Al-CO_3. The presence of Ca^{2+} not only improved the performance of HCl removal by Mg-Al-CO_3, but also expanded the optimal reaction temperature range for HCl removal using hydrotalcite in a CO_2 atmosphere. This expanded temperature range holds great significance for the utilization of remaining heat in subsequent stages of the process. The improved performance can be attributed to several key factors. Firstly, calcium exhibits superior metallicity when compared to magnesium, leading to changes in chemical bonding upon the addition of Ca. The introduction of Ca^{2+} and the formation of new chemical bonds facilitate the interaction and combination with Cl^-. Secondly, the SEM results from Fig.4 B and E reveals significant modifications in the hydrotalcite structure upon the incorporation of Ca. Notably, the layer spacing and size of Ca-Mg-Al-CO_3 was larger in comparison to Mg-Al-CO_3. This structural alteration allows for easier permeation of HCl into the interior of the absorbent, enabling more efficient adsorption and removal of HCl.

3.4 The characterization and mechanism

To further analysis the mechanism underlying the reaction between Ca-Mg-Al-CO_3 and HCl in the presence of CO_2, the XRD patterns of the products were obtained and are presented in Fig. 9.

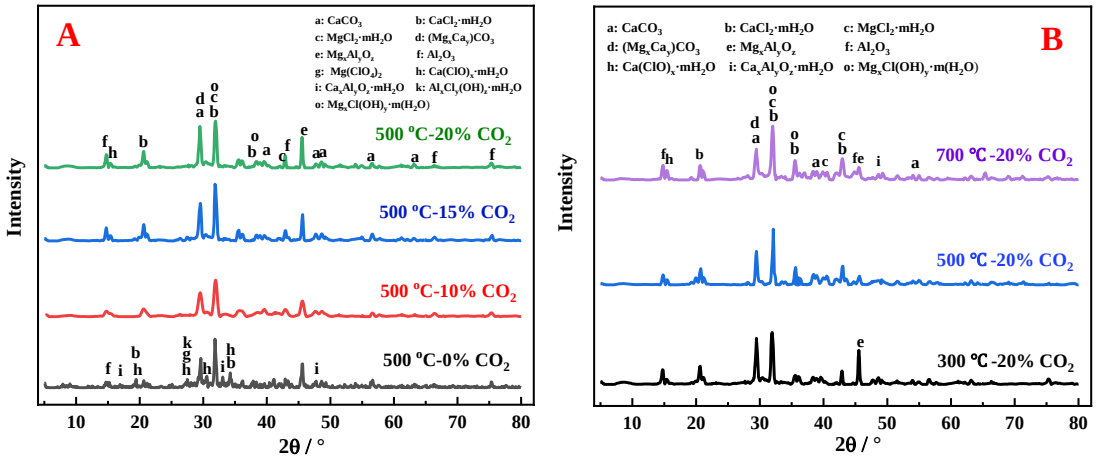

Fig. 9 The XRD patterns of reaction products at different CO_2 concentrations and temperatures (A: the different CO_2 concentrations; B: the different temperatures)

The XRD patterns of the products obtained at 300 ℃ under different CO_2 concentrations are shown in Fig. 9A. A comparison with the XRD patterns of raw Ca-Mg-Al-CO_3 from Fig. 4D reveals a significant decrease in the characteristic diffraction peak of hydrotalcite, indicating its transformation during the reaction. The main products observed were chloride and a mixture of oxidate compounds containing calcium, magnesium, and aluminum, such as $MgCl_2$, $CaCl_2$, Al_2O_3, $Mg_xAl_yO_z$, $Ca_xAl_yO_z$. The presence of metal oxides indicated that they were difficult to react with Cl. The characteristic diffraction peak of CO_3^{2-} containing substance decreased, and in the absence of CO_2, the reaction products included not only Cl^-, but also ClO_x^-. With the increase of CO_2 concentration, the characteristic diffraction peaks of Mg $(ClO_4)_2$, Ca $(ClO)_x$, and Al_xCl_y $(OH)_z$ became weak and eventually disappeared, $CaCl_2$ and $MgCl_2$ became the main products of chloride, indicating that CO_2 influenced the formation of the products during the reaction between HCl and adsorbent. Furthermore, the characteristic diffraction peak of CO_3^{2-} containing substance became stronger, especially that of $CaCO_3$, became stronger, suggesting that Ca^{2+} reacted with CO_2 to generate large particles of $CaCO_3$. This reaction occupied the active sites on the surface of the adsorbent, leading to the formation of a dense layer of $CaCO_3$. Consequently, the diffusion resistance of HCl increased, and the reaction rate between $CaCO_3$ and HCl was slower compared to that between Ca^{2+} and HCl[56, 57]. This phenomenon contributed to the decrease in the performance of HCl removal by the adsorbent. Fig. 9B presents the XRD patterns of the products obtained at a CO_2 concentration of 20 % under different reaction temperatures: 300, 500 and 700 ℃. It can be seen from Fig. 9B that the intensity of the characteristic diffraction peaks

corresponding to carbonates decreased with the increase of temperature, suggesting that the carbonates were prone to decomposition, and the generation of $CaCO_3$ became challenging at high temperatures. Additionally, the peak intensity of $Mg_xAl_yO_z$ became weak, indicating the conversion of $Mg_xAl_yO_z$ into stable compounds such as $MgAl_2O_4$ and Al_2O_3, and these substances didn't react with HCl. Notably, the intensity of the characteristic diffraction peaks of chlorides was more pronounced at 500 ℃ compared to other temperatures. This finding suggests that the adsorption performance of HCl removal was enhanced at 500 ℃. The surface morphology, pore size distribution, and specific surface area of Ca-Mg-Al-CO_3 at different temperatures were shown in Fig.10. As shown in the SEM images of Figure 10A-E, the surface morphology of Ca-Mg-Al-CO_3 becomes increasingly porous as the temperature increases. However, a sintering phenomenon occurs when the temperature exceeds 500 ℃. In Fig.10F, the pores of Ca-Mg-Al-CO_3 are mainly mesopores. With the increase of temperature, the number of pores first increases and then decreases, and pores develop into larger pores, the optimal pore structure is at 500 ºC. Therefore, as shown in Fig. 10G, the specific surface area also first increases and then decreases, the specific surface area was larger at 500 ℃, 58.1 m^2/g. The large specific surface area provides more active sites, facilitating the availability of more active sites. Above results further illustrated that why the Ca-Mg-Al-CO_3 exhibits excellent performance in removing HCl at 500 ºC.

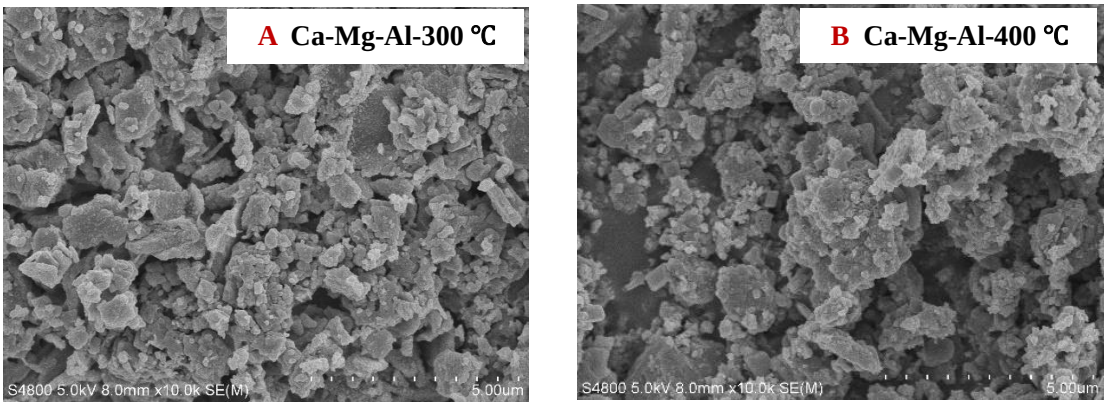

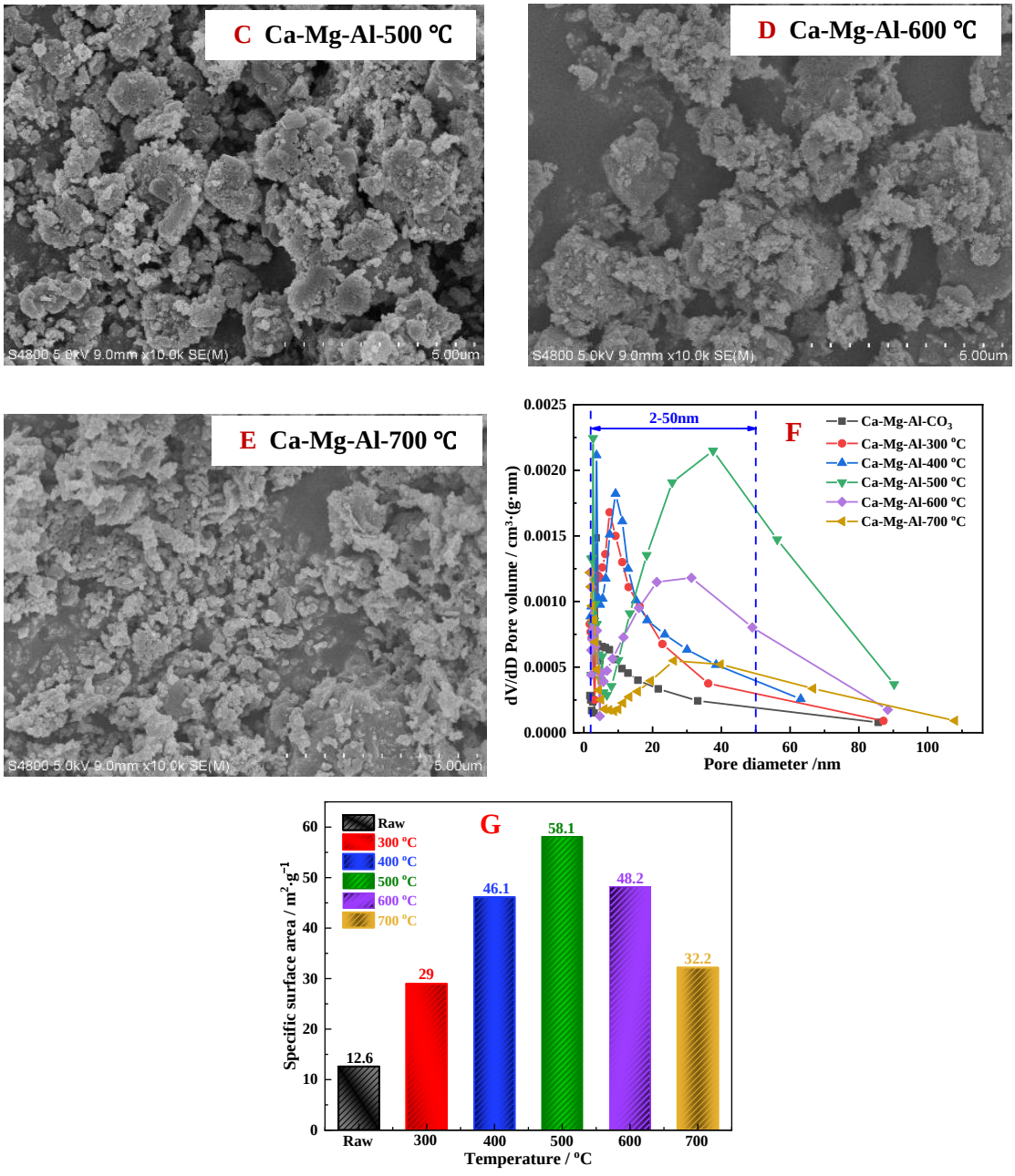

Fig. 10 The surface morphology, pore size distribution, and specifal surface area of Ca-Mg-Al-CO_3 at different temperatures (A-E: Surface morphology; F: Pore size distribution; G: Specific surface area)

3.5 Thermogravimetric experiments

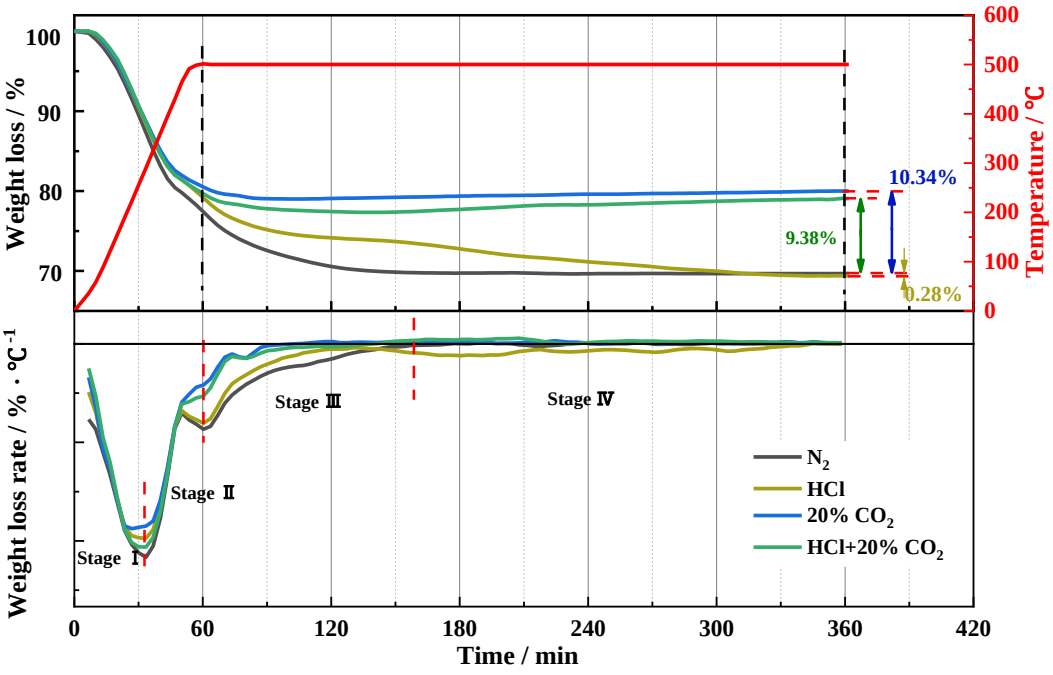

Fig. 11 Adsorption thermogravimetric experiments of HCl and CO_2 by Ca-Mg-Al-CO_3

Fig. 11 displays the TG/DTG curves obtained from - TGA tests conducted on Ca-Mg-Al-CO_3, involving N_2, 400 ppmv HCl, 20 % CO_2, and a mixture of 400 ppmv HCl and 20 % CO_2. The duration of the reaction was 5 hours. During the heating process, the thermogravimetric analyzer followed a linear heating curve, and the temperature stabilized at 500 ℃ after 60 min. Consequently, the reaction gases were introduced at the 60-minute mark, and the reaction continued for 5 h. As shown in the TG curve of N_2, a weight loss of 30.32% was observed. This weight loss primarily consisted of interlayer crystal H_2O and a portion of CO_3^{2-}. The DTG curve of N_2 revealed three distinct stages of weight loss. In stage Ⅰ, which occurred at temperatures below 250 ℃, only interlayer moisture was lost, without affecting the structure of the material. This stage exhibited the highest weight loss peak, with Mg-Al-CO_3 losing 12.7 % of its weight. In stage Ⅱ, as the temperature increased to 250~500 ℃, CO_2 was generated, resulting in the appearance of the second weight loss peak, corresponding to a weight loss of 22.6 %. Stage Ⅲ commenced when the heating temperature reached 500 ℃, with continuous loss of CO_3^{2-} and a

stable weight loss for Ca-Mg-Al-CO_3[41].

Upon introducing HCl gas, an increase in weight was observed compared to the N_2 condition, indicating a rapid adsorption stage for HCl. In the DTG curve, four weight loss peaks were observed in the stage Ⅲ and Ⅳ. This phenomenon can be explained by the reaction of HCl with the metals present on the adsorbent's surface, resulting in an increase in weight. Consequently, the weight loss rate slowed down due to these chemical reactions. The chemical reaction equations for this process are shown in *React*. 2 and 3 (M represents metal). as the reaction time increased, the active sites available for HCl adsorption became occupied. At this stage, Cl^- entered the interior of the adsorbent through the pores, replacing undecomposed CO_3^{2-}, and this process is illustrated by *React*. 4, which represents the main reaction pathway in this stage. As the molecular weight of Cl^- was less than that of CO_2, the weight loss decreased rapidly. Consequently, the overall weight loss reached 30.6%, which represented a decrease of 28 % compared to the TG curve of N_2.

In the presence of 20 % CO_2, an increase in weight was observed upon introducing CO_2. The weight increase was greater than that observed in the HCl gas condition, and it was the highest among the four TG curves, indicating a stronger adsorption capacity for CO_2. In the DTG curve, three peaks of weight increase were observed in the stage Ⅲ and Ⅳ, providing further evidence of the CO_2 adsorption process. Comparing it with the TG curve of N_2, the ultimate weight increased by 10.34 %. This increase can be attributed to the reaction between the adsorbent and CO_2, leading to the formation of new carbonates, primarily $CaCO_3$, as shown in Fig. 9.

In the presence of 20 % CO_2 and 400 ppmv HCl, the TG curve showed a final weight increase of 9.38 % compared to the product in N_2. In the DTG curve, there was a loss weight peak in stage Ⅲ, mainly caused by HCl gas, as observed in the DTG curve of 20 % CO_2. Subsequently, there

were two weight increase peaks in stage Ⅳ, caused by CO_2 gas. These results indicated a competitive relationship between HCl and CO_2 during the reaction process, the reaction rate of the adsorbent with HCl was faster than that of CO_2 in the early stage, and the adsorption capacity for CO_2 was stronger than for HCl. This can be attributed to the significantly higher concentration of CO_2 compared to HCl. This competitive relationship explains the performance of HCl removal using Ca-Mg-Al-CO_3 in the presence of CO_2.

$$M^{2+}+2Cl^- \rightarrow MCl_2 \quad (React.\ 2)$$

$$M^{2+}+xCl^- +xO^{2-} \rightarrow M(ClO)_x \quad (React.\ 3)$$

$$Ca_{3n}Mg_nAl_{4n/3}(OH)_{16n/3}(CO_3)_{2n/3}\bullet mH_2O + 4n/3\ HCl \rightarrow Ca_{3n}Mg_nAl_{4n/3}(OH)_{16n/3}Cl_{4n/3} + 2n/3\ CO_2 + (m + 2n/3)H_2O \quad (React.\ 4)$$

3.6 Apparent adsorption kinetic

The apparent adsorption kinetic models mainly include kinetic control type and diffusion control type. The diffusion control type includes Intra-particle diffusion model, which describes gas film or intra-particle diffusion as a rate-controlling step. The commonly used kinetic control models are Pseudo-first-order model (PFO), Pseudo-second-order model (PSO), Elovich model and Bangham model, all of which describe the kinetic adsorption process of surface adsorption or surface chemical reactions as rate-controlling steps. The experimental results of HCl removal by Ca-Mg-Al-CO_3 at different CO_2 concentrations were analyzed using the above models, and the fitting results of adsorption kinetics are presented in Fig. 12.

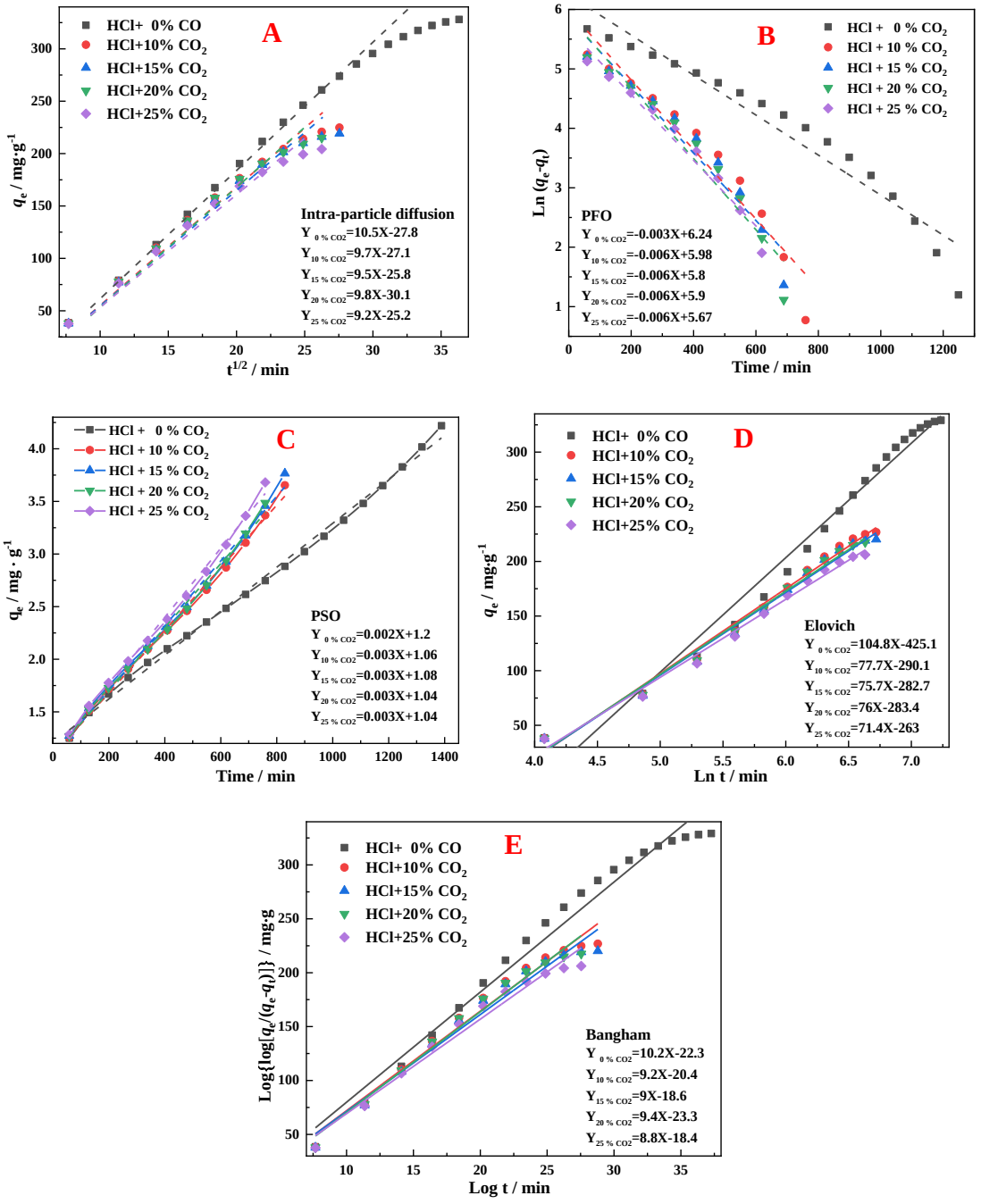

Fig. 12 The fitting results of different adsorption kinetic model (A: Intra-particle diffusion model; B: Pseudo-first-order model (PFO), C: Pseudo-second-order model; D: Elovich model; E: Bangham model)

As depicted in Fig. 12 and the correlation coefficients (R^2) summarized in Table 2, based on the fitting result of the intra-particle diffusion model, the fitted line does not pass through the origin and did not exhibit a linear relationship, the R^2 values are more than 0.98, indicating that diffusion

control is not the solely governed by single rate-determining steps. The fitting results of 4 kinetic control types showed a relatively best agreement with the PSO model, the R^2 values exceed 0.99. The result illustrates that the chemical adsorption is main reaction mechanism in whole reaction process, and chemical adsorption involves electron sharing or electron transfer between Ca-Mg-Al-CO_3 and HCl, CO_2. Compared to PSO model. Although the R^2 values of other 3 adsorption kinetic models were slightly lower than that of the PSO model, all models exhibited correlation coefficients above 0.97, as shown in Fig. 12B, D and E, there a good fitting result in the early stage of the reaction, indicating it is controlled by multiple control steps in the early stage of the reaction.

Table. 2 The correlation coefficients (R^2) of different adsorption kinetic models

Model	0% CO_2 +HCl	10% CO_2 + HCl	15% CO_2 + HCl	20% CO_2 +HCl	25% CO_2 +HCl
Intra-particle diffusion	0.983	0.985	0.983	0.987	0.985
PFO	0.94	0.933	0.946	0.943	0.968
PSO	0.996	0.996	0.994	0.996	0.996
Elovich	0.98	0.988	0.987	0.989	0.99
Bangham	0.977	0.976	0.972	0.978	0.974

4. Conclusions

In this study, the performance of HCl removal using Mg-Al-CO_3 and Ca-Mg-Al-CO_3, as modified sorbent, in the presence of CO_2 were investigated.

The Ca-Mg-Al-CO_3 was successfully synthesized with a larger layer spacing d_{003} and particle size compared to Mg-Al-CO_3. CO_2 had a positive impact on the removal of HCl using Mg-Al-CO_3, but a negative impact on the removal of HCl using Ca-Mg-Al-CO_3. However, the performance of HCl removal using Ca-Mg-Al-CO_3 was superior to that of Mg-Al-CO_3. The main reason for this difference is that CO_2 can react with Mg-Al-CO_3 to generate new hydrotalcite intercalated anions through a regeneration process, thereby enhancing the performance of HCl removal. In contrast,

Ca-Mg-Al-CO_3 reacted with CO_2 to form large particles of $CaCO_3$, which not only occupied the active sites but also hindered the reaction between HCl and the adsorbent, leading to a decrease in the performance of HCl removal. The main products of reaction between Ca-Mg-Al-CO_3 and HCl were $CaCl_2$ and $MgCl_2$. The presence of CO_2 plays a competitive role in the removal of HCl. The adsorption rate of HCl was initially faster than that of CO_2, but the adsorption capacity of CO_2 was stronger. This can be attributed to the significantly higher concentration of CO_2 compared to HCl. The adsorption reactions of HCl and CO_2 by Ca-Mg-Al-CO_3 was controlled by multiple rate-controlling mechanisms in the early stage of the reaction, and follow a PSO model in the whole process. The study demonstrates that Ca-Mg-Al-CO_3 exhibits excellent performance in removing HCl, which is of significant importance for achieving high-quality synthesis gas and further promoting pyrolysis gasification technology. The findings have academic and industrial significance in advancing waste-to-energy conversion technologies and contributing to the reduction of carbon emissions.

Credit author statement

Songshan Cao: Investigation, Methodology, Writing - original draft. Jun Cao: Writing - review & editing, Funding acquisition. Hualun Zhu: Writing - review & editing. Yaji Huang: Supervision. Baosheng Jin: Supervision, Funding acquisition. Massimiliano Materazzi: Supervision, Writing - review & editing.

Acknowledgements

This work was supported by National Natural Science Foundation of China (52076067), the Natural Science Foundation of Jiangsu Province (BK20201319), Carbon Peak and Carbon Neutrality Science Technology Innovation Special Funds (Major Scientific and Technological Achievements Transformation) Project of Jiangsu Province (SBA2022080063), and the Postgraduate Research & Practice Innovation Program of Jiangsu Province (KYCX20_0097).

References:

[1] S. Vyas, P. Prajapati, A.V. Shah, S. Varjani, Municipal solid waste management: Dynamics, risk assessment, ecological influence, advancements, constraints and perspectives, Science of The Total Environment, 814 (2022) 152802.

[2] E. Garcia, I.F. Ejim, H. Liu, Thermogravimetric analysis of co-combustion of a bituminous coal and coffee industry by-products, Thermochimica acta, 715 (2022) 179296.

[3] A. Krishnan, A. Nighojkar, B. Kandasubramanian, Emerging towards zero carbon footprint via carbon dioxide capturing and sequestration, Carbon Capture Science & Technology, (2023) 100137.

[4] A.T. Hoang, H.C. Ong, I.R. Fattah, C.T. Chong, C.K. Cheng, R. Sakthivel, Y.S. Ok, Progress on the lignocellulosic biomass pyrolysis for biofuel production toward environmental sustainability, Fuel Processing Technology, 223 (2021) 106997.

[5] M. Materazzi, P.U. Foscolo, The role of waste and renewable gas to decarbonize the energy sector, in: Substitute natural gas from waste, Elsevier, 2019, pp. 1-19.

[6] M. Materazzi, M. Materazzi, Gasification of waste derived fuels in fluidized beds: Fundamental aspects and industrial challenges, Clean Energy from Waste: Fundamental Investigations on Ashes and Tar Behaviours in a Two Stage Fluid Bed-Plasma Process for Waste Gasification, (2017) 19-63.

[7] R. Nandhini, D. Berslin, B. Sivaprakash, N. Rajamohan, D.-V.N. Vo, Thermochemical conversion of municipal solid waste into energy and hydrogen: a review, Environmental Chemistry Letters, 20 (2022) 1645-1669.

[8] D. Li, J. Yang, Y. Zhao, H. Yuan, Y. Chen, Ultra-highly porous carbon from Wasted soybean residue with tailored porosity and doped structure as renewable multi-purpose absorbent for

638 efficient CO_2, toluene and water vapor capture, Journal of Cleaner Production, 337 (2022) 130283.
639 [9] E. Skountzos, C.A. Price, M.M. Alsalem, S.G. Booth, S. Polastri, S.A. Cussen, C.M. Parlett,
640 K.L.S. Campbell, Use of copper carbonate as corrosion inhibitor for carbon steel in post
641 combustion carbon capture, Carbon Capture Science & Technology, 6 (2023) 100095.
642 [10] S. Sun, Z. Lv, Y. Qiao, C. Qin, S. Xu, C. Wu, Integrated CO_2 capture and utilization with
643 CaO-alone for high purity syngas production, Carbon Capture Science & Technology, 1 (2021)
644 100001.
645 [11] M. Sajid, A. Raheem, N. Ullah, M. Asim, M.S. Ur Rehman, N. Ali, Gasification of municipal
646 solid waste: Progress, challenges, and prospects, Renewable and Sustainable Energy Reviews, 168
647 (2022) 112815.
648 [12] Ö. Tezer, N. Karabağ, A. Öngen, C.Ö. Çolpan, A. Ayol, Biomass gasification for sustainable
649 energy production: A review, International Journal of Hydrogen Energy, 47 (2022) 15419-15433.
650 [13] H. Zhu, Z. Chen, L. Pastor-Perez, X. Long, M. Millan, How syngas composition affects
651 catalytic steam reforming of tars: An analysis using toluene as model compound, International
652 Journal of Hydrogen Energy, 48 (2023) 1290-1303.
653 [14] Y. Zhang, J. Huang, P.T. Williams, Fe–Ni–MCM-41 catalysts for hydrogen-rich syngas
654 production from waste plastics by pyrolysis–catalytic steam reforming, Energy & Fuels, 31 (2017)
655 8497-8504.
656 [15] T. Chen, J. Cao, B. Jin, Oxygen-Enriched Gasification of Dried Sewage Sludge, Refuse-
657 Derived Fuel, and Their Cogasification in a Laboratory-Scale Fluidized Bed, Industrial &
658 Engineering Chemistry Research, 58 (2018) 479-486.
659 [16] Y. Xie, L. Wang, H. Li, L.J. Westholm, L. Carvalho, E. Thorin, Z. Yu, X. Yu, Ø. Skreiberg, A

660 critical review on production, modification and utilization of biochar, Journal of Analytical and
661 Applied Pyrolysis, 161 (2022) 105405.
662 [17] J. Qin, Y. Zhang, S. Heberlein, G. Lisak, Y. Yi, Characterization and comparison of
663 gasification and incineration fly ashes generated from municipal solid waste in Singapore, Waste
664 Management, 146 (2022) 44-52.
665 [18] G. Liu, H. Wang, S. Deplazes, A. Veksha, C. Wirz-Töndury, A. Giannis, T.T. Lim, G. Lisak,
666 Ba–Al-decorated iron ore as bifunctional oxygen carrier and HCl sorbent for chemical looping
667 combustion of syngas, Combustion and Flame, 223 (2021) 230-242.
668 [19] H.L. Zhu, L. Pastor-Pérez, M. Millan, Catalytic steam reforming of toluene: Understanding
669 the influence of the main reaction parameters over a reference catalyst, Energies, 13 (2020) 813.
670 [20] S.K. Awasthi, S. Sarsaiya, V. Kumar, P. Chaturvedi, R. Sindhu, P. Binod, Z. Zhang, A. Pandey,
671 M.K. Awasthi, Processing of municipal solid waste resources for a circular economy in China: An
672 overview, Fuel, 317 (2022) 123478.
673 [21] S. Heberlein, W.P. Chan, A. Veksha, A. Giannis, L. Hupa, G. Lisak, High temperature
674 slagging gasification of municipal solid waste with biomass charcoal as a greener auxiliary fuel,
675 Journal of Hazardous Materials, 423 (2022) 127057.
676 [22] Y. Ren, C. Cao, H. Hu, S. Lei, X. Yuan, X. Li, H. Yao, Transformation behavior and fate of
677 chlorine in polychloroprene (PCP) during its pyrolysis, Fuel, 317 (2022) 123573.
678 [23] J. Bei, X. Xu, M. Zhan, X. Li, W. Jiao, L. Khachatryan, A. Wu, Revealing the Mechanism of
679 Dioxin Formation from Municipal Solid Waste Gasification in a Reducing Atmosphere,
680 Environmental Science & Technology, 56 (2022) 14539-14549.
681 [24] Y. Zhao, G. Liu, J. Huang, A. Veksha, X. Wu, A. Giannis, T.T. Lim, G. Lisak, Sorbents for

682 high-temperature removal of alkali metals and HCl from municipal solid waste derived syngas,
683 Fuel, 321 (2022) 124058.
684 [25] G. Yuan, W. Zhou, R. Yang, Y. Liu, J. Zhu, K. Yin, D. Chen, Acid Gas and Tar Removal from
685 Syngas of Refuse Gasification by Catalytic Reforming, Catalysts, 12 (2022) 1519.
686 [26] Y. Li, X. Li, H. Wang, T. Yang, R. Li, Gas phase migration of Cl during thermal conversion of
687 municipal solid waste, Energy Sources, Part A: Recovery, Utilization, and Environmental Effects,
688 42 (2020) 153-160.
689 [27] S. Liang, Z. Fan, W. Zhang, M. Guo, F. Cheng, M. Zhang, Inexpensive metal oxides
690 nanoparticles doped Na_2CO_3 fibers for highly selective capturing trace HCl from HCl/CO_2
691 mixture gas at low temperature, Chemical Engineering Journal, 352 (2018) 634-643.
692 [28] B. Dou, C. Wang, H. Chen, Y. Song, B. Xie, Y. Xu, C. Tan, Research progress of hot gas
693 filtration, desulphurization and HCl removal in coal-derived fuel gas: A review, Chemical
694 Engineering Research and Design, 90 (2012) 1901-1917.
695 [29] M.-T. Lee, Z.-Q. Wang, J.-R. Chang, Activated-carbon-supported NaOH for removal of HCl
696 from reformer process streams, Industrial & engineering chemistry research, 42 (2003) 6166-6170.
697 [30] Z.-S. Liu, M.-Y. Wey, C.-L. Lin, Reaction characteristics of Ca (OH) $_2$, HCl and SO_2 at low
698 temperature in a spray dryer integrated with a fabric filter, Journal of hazardous materials, 95
699 (2002) 291-304.
700 [31] U. Sikander, S. Sufian, M. Salam, A review of hydrotalcite based catalysts for hydrogen
701 production systems, International journal of hydrogen energy, 42 (2017) 19851-19868.
702 [32] S. Nishimura, A. Takagaki, K. Ebitani, Characterization, synthesis and catalysis of
703 hydrotalcite-related materials for highly efficient materials transformations, Green Chemistry, 15

(2013) 2026-2042.

[33] E. Bernard, W.J. Zucha, B. Lothenbach, U. Mäder, Stability of hydrotalcite (Mg-Al layered double hydroxide) in presence of different anions, Cement and Concrete Research, 152 (2022) 106674.

[34] L.-X. Zhao, J.-L. Liang, N. Li, H. Xiao, L.-Z. Chen, R.-S. Zhao, Kinetic, thermodynamic and isotherm investigations of Cu^{2+} and Zn^{2+} adsorption on LiAl hydrotalcite-like compound, Science of The Total Environment, 716 (2020) 137120.

[35] L.K.G. Bhatta, S. Subramanyam, M.D. Chengala, S. Olivera, K. Venkatesh, Progress in hydrotalcite like compounds and metal-based oxides for CO_2 capture: a review, Journal of Cleaner Production, 103 (2015) 171-196.

[36] T. Kameda, T. Yoshioka, T. Hoshi, M. Uchida, A. Okuwaki, Treatment of hydrochloric acid with magnesium–aluminum oxide at ambient temperatures, Separation and purification technology, 51 (2006) 272-276.

[37] N. Iyi, T. Matsumoto, Y. Kaneko, K. Kitamura, Deintercalation of carbonate ions from a hydrotalcite-like compound: Enhanced decarbonation using acid− salt mixed solution, Chemistry of materials, 16 (2004) 2926-2932.

[38] T. Kameda, Y. Takahashi, S. Kumagai, Y. Saito, S. Fujita, I. Itou, T. Han, T. Yoshioka, Comparison of Mg–Al layered double hydroxides intercalated with OH^- and CO_3^{2-} for the removal of HCl, SO_2, and NO_2, Journal of Porous Materials, 29 (2022) 723-728.

[39] T. Kameda, H. Uchida, S. Kumagai, Y. Saito, K. Mizushina, I. Itou, T. Han, T. Yoshioka, Desorption of Cl^- from Mg-Al layered double hydroxide intercalated with Cl^- using CO_2 gas and water, Chinese Journal of Chemical Engineering, 29 (2021) 131-134.

[40] J. Cao, T. Chen, B. Jin, Y. Huang, C. Hu, Structural effects of HCl adsorption on Mg–Fe hydrotalcite-like oxides at 350–650 C in flue gas, Industrial & Engineering Chemistry Research, 57 (2018) 14939-14947.

[41] J. Cao, T. Chen, B. Jin, Y. Huang, C. Hu, Adsorption of HCl on calcined Ca and Zn hydrotalcite-like compounds (HTLs) at medium-high temperature in flue gas, Industrial & Engineering Chemistry Research, 58 (2018) 18-26.

[42] J. Chen, Y. Xu, P. Liao, H. Wang, H. Zhou, Recent progress in integrated CO_2 capture and conversion process using dual function materials: a state-of-the-art review, Carbon Capture Science & Technology, 4 (2022) 100052.

[43] Y. Xu, M. Wu, X. Yang, S. Sun, Q. Li, Y. Zhang, C. Wu, R.E. Przekop, E. Romańczuk-Ruszuk, D. Pakuła, Recent advances and prospects in high purity H_2 production from sorption enhanced reforming of bio-ethanol and bio-glycerol as carbon negative processes: A review, Carbon Capture Science & Technology, (2023) 100129.

[44] T. Jiang, F. Xiao, Y. Zhao, S. Wang, X. Ma, High-temperature CO_2 sorbents with citrate and stearate intercalated CaAl hydrotalcite-like as precursor, Chinese Journal of Chemical Engineering, 50 (2022) 177-184.

[45] Z.-z. Yang, J.-j. Wei, G.-m. Zeng, H.-q. Zhang, X.-f. Tan, C. Ma, X.-c. Li, Z.-h. Li, C. Zhang, A review on strategies to LDH-based materials to improve adsorption capacity and photoreduction efficiency for CO_2, Coordination Chemistry Reviews, 386 (2019) 154-182.

[46] K. Bo, Y. Feng, Z. Lan, W. Yang, Y. Li, Facile Preparation of Porous CaMgAl Hydrotalcite-Like Derived Mixed Oxides through Alkaline Etching of KOH for CO_2 Capture, Russian Journal of Physical Chemistry A, 96 (2022) 1555-1560.

748 [47] Y. Feng, B. Xiao, K. Bo, H. Chen, W. Yang, Controllable preparation of porous Ca-Mg-Al
749 hydroxides based adsorbents and their CO_2 adsorption performances, Ferroelectrics, 594 (2022)
750 44-56.
751 [48] Y. Li, W. Wang, X. Cheng, M. Su, X. Ma, X. Xie, Simultaneous CO_2/HCl removal using
752 carbide slag in repetitive adsorption/desorption cycles, Fuel, 142 (2015) 21-27.
753 [49] X. Xie, Y.-J. Li, C.-T. Liu, W.-J. Wang, HCl absorption by CaO/$Ca_3Al_2O_6$ sorbent from CO_2
754 capture cycles using calcium looping, Fuel Processing Technology, 138 (2015) 500-508.
755 [50] S. Cao, J. Cao, H. Zhu, Y. Huang, B. Jin, M. Materazzi, Removal of HCl from gases using
756 modified calcined Mg-Al-CO_3 hydrotalcite: Performance, mechanism, and adsorption kinetics,
757 Fuel, 355 (2024) 129445.
758 [51] V.S. Mane, I.D. Mall, V.C. Srivastava, Kinetic and equilibrium isotherm studies for the
759 adsorptive removal of Brilliant Green dye from aqueous solution by rice husk ash, Journal of
760 environmental management, 84 (2007) 390-400.
761 [52] R. Ezzati, Derivation of pseudo-first-order, pseudo-second-order and modified pseudo-first-
762 order rate equations from Langmuir and Freundlich isotherms for adsorption, Chemical
763 Engineering Journal, 392 (2020) 123705.
764 [53] M.A. Hubbe, S. Azizian, S. Douven, Implications of apparent pseudo-second-order
765 adsorption kinetics onto cellulosic materials: A review, BioResources, 14 (2019).
766 [54] S.Y. Elovich, O. Larinov, Theory of adsorption from solutions of non electrolytes on solid (I)
767 equation adsorption from solutions and the analysis of its simplest form,(II) verification of the
768 equation of adsorption isotherm from solutions, Izv. Akad. Nauk. SSSR, Otd. Khim. Nauk, 2
769 (1962) 209-216.

770 [55] C. Aharoni, S. Sideman, E. Hoffer, Adsorption of phosphate ions by collodion- coated
771 alumina, Journal of Chemical Technology and Biotechnology, 29 (1979) 404-412.
772 [56] C. Chi, Y. Li, R. Sun, X. Ma, L. Duan, Z. Wang, HCl removal performance of Mg-stabilized
773 carbide slag from carbonation/calcination cycles for CO_2 capture, RSC advances, 6 (2016)
774 104303-104310.
775 [57] B. Shemwell, Y.A. Levendis, G.A. Simons, Laboratory study on the high-temperature capture
776 of HCl gas by dry-injection of calcium-based sorbents, Chemosphere, 42 (2001) 785-796.

Conflict of Interest

The authors declare that they have no known competing financial interests or personal relationships that could have appeared to influence the work reported in this paper.

Author statement

Songshan Cao: Investigation, Methodology, Writing - original draft. Jun Cao: Writing - review & editing, Funding acquisition. Hualun Zhu: Writing - review & editing. Yaji Huang: Supervision. Baosheng Jin: Supervision, Funding acquisition. Massimiliano Materazzi: Supervision, Writing - review & editing.